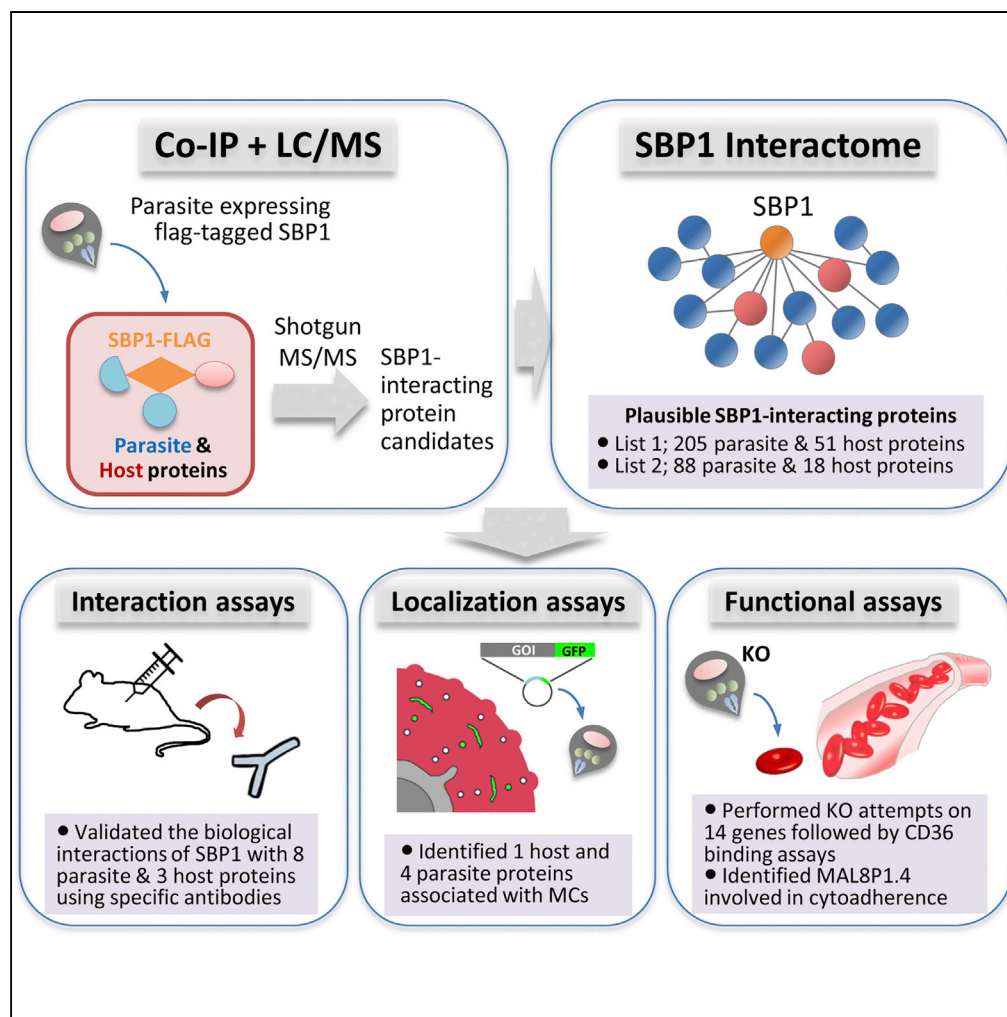


## Article

# A High-Resolution Map of SBP1 Interactomes in *Plasmodium falciparum*-infected Erythrocytes



Ryo Takano,  
Hiroko Kozuka-  
Hata, Daisuke  
Kondoh, Hiroki  
Bochimoto,  
Masaaki Oyama,  
Kentaro Kato

kkato@obihiro.ac.jp

## HIGHLIGHTS

We used shotgun proteomics to identify SBP1-interacting factors

System validation showed complex interplay between parasite and host proteins

Our system can be used to explore protozoan parasite virulence in erythrocytes

## Article

# A High-Resolution Map of SBP1 Interactomes in *Plasmodium falciparum*-infected Erythrocytes

Ryo Takano,<sup>1</sup> Hiroko Kozuka-Hata,<sup>2</sup> Daisuke Kondoh,<sup>3</sup> Hiroki Bochimoto,<sup>4</sup> Masaaki Oyama,<sup>2</sup> and Kentaro Kato<sup>1,5,6,\*</sup>

## SUMMARY

The pathogenesis of malaria parasites depends on host erythrocyte modifications that are facilitated by parasite proteins exported to the host cytoplasm. These exported proteins form a trafficking complex in the host cytoplasm that transports virulence determinants to the erythrocyte surface; this complex is thus essential for malaria virulence. Here, we report a comprehensive interaction network map of this complex. We developed authentic, unbiased, highly sensitive proteomic approaches to determine the proteins that interact with a core component of the complex, SBP1 (skeleton-binding protein 1). SBP1 interactomes revealed numerous exported proteins and potential interactors associated with SBP1 intracellular trafficking. We identified several host-parasite protein interactions and linked the exported protein MAL8P1.4 to *Plasmodium falciparum* virulence in infected erythrocytes. Our study highlights the complicated interplay between parasite and host proteins in the host cytoplasm and provides an interaction dataset connecting dozens of exported proteins required for *P. falciparum* virulence.

## INTRODUCTION

Malaria remains one of the world's most important infectious diseases, affecting ~200 million people worldwide annually (WHO, 2018). When *Plasmodium falciparum*, one of the most virulent forms of the human malaria parasite, establishes infection in host erythrocytes, the parasites export numerous proteins to the host cell's cytoplasm and plasma membrane to drastically remodel the host cell (Hiller et al., 2004; Maier et al., 2009). These exported proteins are collectively referred to as the exportome, and some of these proteins form a large protein complex that leads to profound structural and morphological changes in the host erythrocytes (LaCount et al., 2005); for example, Maurer's clefts (Lanzer et al., 2006) and knobs (Wickham et al., 2001) are established in the cytoplasm and on the surface of erythrocytes, respectively. Consequently, the infected erythrocytes become more rigid and adhere to the vascular endothelium, which prevents clearance of the infected erythrocytes by the spleen and subsequently disrupts normal blood flow, resulting in severe malaria in humans (De Niz et al., 2016; Maier et al., 2008).

The adherence of infected erythrocytes to the vascular endothelium is mediated by interactions between parasite adhesins on the erythrocyte surface and host endothelial receptors (Fairhurst et al., 2005; Janes et al., 2011; Waller et al., 2003). *Plasmodium falciparum* erythrocyte membrane protein 1 (PfEMP1) is an antigenically variant adhesin that is transported to knobs on the erythrocyte surface (Waller et al., 1999). Knobs are macromolecular complexes of knob-associated histidine-rich protein (KAHRP) that anchor PfEMP1 to the membrane skeleton (Oh et al., 2000; Waller et al., 1999). In contrast, Maurer's clefts are involved in the trafficking of PfEMP1 to the erythrocyte surface (Lanzer et al., 2006; Maier et al., 2008; Wickham et al., 2001). Many exported proteins, represented by skeleton-binding protein 1 (SBP1) (Cooke et al., 2006; Maier et al., 2007), membrane-associated histidine-rich protein 1 (MAHRP1) (Spycher et al., 2008), ring-exported protein 1 (REX1) (Hanssen et al., 2008), subtelomeric variant open reading frame (STEVOR) (Przyborski et al., 2005), and PfEMP1-trafficking protein 1 and 5 (PTP1 and PTP5) (Maier et al., 2008; Rug et al., 2014), have been shown to reside in Maurer's clefts. Some of these exported proteins are essential for the intracellular transport of PfEMP1 to the erythrocyte surface, suggesting that they form a large protein complex in the Maurer's clefts that serves as protein-trafficking machinery to transport exported proteins to their final destinations (Rug et al., 2014). However, essential information regarding the interactions between these exported proteins is lacking, because of the technical difficulties of

<sup>1</sup>National Research Center for Protozoan Diseases, Obihiro University of Agriculture and Veterinary Medicine, Inada-cho, Obihiro, Hokkaido 080-8555, Japan

<sup>2</sup>Medical Proteomics Laboratory, Institute of Medical Science, The University of Tokyo, Minato-ku, Tokyo 108-8639, Japan

<sup>3</sup>Laboratory of Veterinary Anatomy, Department of Basic Veterinary Medicine, Obihiro University of Agriculture and Veterinary Medicine, Inada-cho, Obihiro, Hokkaido 080-8555, Japan

<sup>4</sup>Health Care Administration Center, Obihiro University of Agriculture and Veterinary Medicine, Inada-cho, Obihiro, Hokkaido 080-8555, Japan

<sup>5</sup>Laboratory of Sustainable Animal Environment, Graduate School of Agricultural Science, Tohoku University, Naruko-onsen, Osaki, Miyagi 989-6711, Japan

<sup>6</sup>Lead Contact

\*Correspondence: [kkato@obihiro.ac.jp](mailto:kkato@obihiro.ac.jp)

<https://doi.org/10.1016/j.isci.2019.07.035>



studying protein-protein interactions in the cytoplasm of erythrocytes infected with *Plasmodium falciparum* (Batinovic et al., 2017; Rug et al., 2014).

The *P. falciparum* exportome had been predicted to comprise approximately 400 proteins since the discovery of a motif sequence called PEXEL (*P. falciparum* exported elements) or HT (host-targeting sequence), which is conserved at the N-terminal end of many exported proteins (Hiller et al., 2004; Marti et al., 2004). However, a previous study also identified the presence of many proteins that lack the canonical PEXEL/HT motif but could be efficiently exported to host cytoplasm (Heiber et al., 2013), thereby complicating the identification of the exported proteins that comprise the *P. falciparum* exportome. These PEXEL-negative exported proteins (PNEPs) include SBP1, MAHRP1, and REX1, all of which are related to and are indispensable for malaria virulence (Cooke et al., 2006; Hanssen et al., 2008; Maier et al., 2007; Spycher et al., 2008). Given the difficulty to predict and identify PNEPs based on protein sequences, an alternative approach is needed to directly identify PNEPs based on protein-protein interactions in the host cytoplasm.

In this study, we developed an alternative proteomic approach to identify exported proteins involved in the trafficking complex and to clarify the *P. falciparum* exportome. Highly sensitive mass spectrometry identified multiple proteins that interact with SBP1 through its intraerythrocytic-trafficking process. Further interaction, localization, and functional assays demonstrated that the SBP1 interactomes established in our study represent a powerful and invaluable platform to identify exported proteins related to severe malaria caused by *P. falciparum*.

## RESULTS

### A High-Resolution Map of SBP1 Interactomes

To identify proteins that interact with SBP1, we performed FLAG-tag-based immunoprecipitations with lysates of erythrocytes infected with parasites overexpressing C-terminally FLAG-tagged SBP1 (SBP1-FLAG), and analyzed the co-immunoprecipitated proteins by mass spectrometry (Gorai et al., 2012; Watanabe et al., 2014). We first generated parasites episomally expressing SBP1-FLAG and confirmed that the FLAG-tagged SBP1 retained the localization of wild-type SBP1 in Maurer's clefts (Figures 1A and 1B).

Human erythrocytes were infected with 3D7 wild-type parasites, or parasites expressing SBP1-FLAG, and late trophozoite or schizont-enriched red blood cells (RBCs) were purified via Percoll gradient centrifugation and magnetic isolation. Whole-cell lysates were prepared, immunoprecipitated with an anti-FLAG antibody, and subjected to SDS-PAGE followed by western blot and silver staining. Although the bait protein was detected among the precipitants from the lysates of RBCs infected with SBP1-FLAG-expressing parasites (Figure 1C), multiple proteins were non-specifically bound to the immunoprecipitation beads and specific bands for immunoprecipitates from the SBP1-FLAG samples were not detected (Figure 1D). We, therefore, employed a highly sensitive shotgun proteomic approach, and compared the proteomes of the two precipitates. The SBP1-FLAG and 3D7 proteomes contained 1,381 and 1,367 proteins, respectively, with 1,125 (~81%) overlapping proteins (Figure 1E and Table S1). No statistically significant differences were observed in the power of protein detection or protein coverage between the two proteomes, indicating that the proteomes were comparable (Figures 1F and 1G). A total of 256 proteins, 51 host and 205 parasite proteins, was specifically detected in only the SBP1-FLAG proteome (Figure 1E); however, these included many proteins with a relatively low Mascot protein score (Table S2).

We then refined the list of proteins based on a comparison of their Mascot protein scores and identified 106 proteins (88 parasite and 18 host proteins) that specifically co-immunoprecipitated with SBP1 (Figure 1H and Table S3; details are provided in the Transparent Methods). In addition to spectrin (SPTA1 and SPTB), a host factor known to interact with SBP1 (Blisnick et al., 2000; Kats et al., 2015), we identified several parasite proteins, including PfEMP1, PfESP2, and PTP1, all of which form a large protein complex with SBP1 inside host cells (Batinovic et al., 2017; Cooke et al., 2006; Maier et al., 2007; Mbengue et al., 2015; Rug et al., 2014), as top-ranked hit proteins, thereby demonstrating the reliability of our approach relative to previous studies (Figure 1I).

We next performed a functional enrichment analysis (Wang et al., 2015) and categorized the potential SBP1 interactors according to subcellular compartments. Gene Ontology (GO) analysis identified Maurer's clefts (Benjamini-adjusted  $p = 1.6 \times 10^{-4}$ ), and the cytoskeleton (Benjamini-adjusted  $p = 0.032$ ) as the most enriched by parasite and host proteins, respectively (Figure 2A). In addition, most of the high-ranked GO

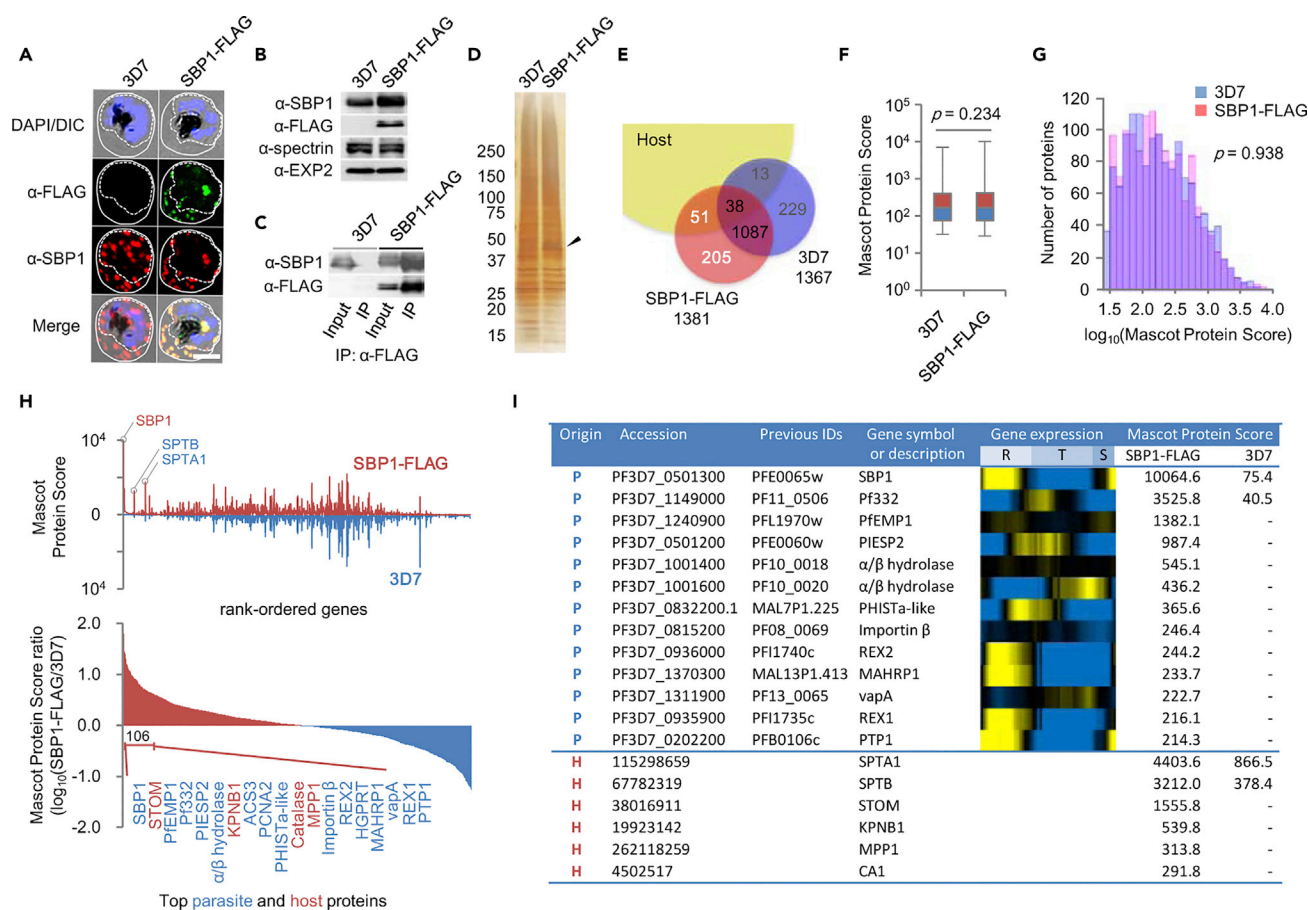


**Figure 1. An Unbiased Comparative Proteomic Approach to Identifying Proteins That Interact with SBP1**

(A) Immunofluorescence assay on 3D7/SBP1-FLAG cells: the FLAG signal (green) co-localizes with that of endogenous protein (SBP1; red). Erythrocyte and parasitophorous vacuole membranes are circled by solid and dotted lines, respectively. Scale bar, 3  $\mu$ m. (B) Western blot analysis of 3D7/SBP1-FLAG cells: parasite-infected RBCs were purified by magnetic-activated cell sorting (MACS), lysed with SDS/Triton lysis buffer, and equivalent amounts of samples were analyzed by western blot. (C and D) (C) Western blot and (D) silver stain analyses of proteins co-immunoprecipitated with SBP1-FLAG. The arrow indicates a bait protein (SBP1-FLAG). (E) Venn diagram comparing proteins identified in 3D7 and SBP1-FLAG proteomes. A total of 256 proteins were specifically detected in the SBP1-FLAG proteome. (F and G) (F) Average and (G) distribution of Mascot Protein Scores of proteins in two proteomic datasets. P values were calculated by using Mann-Whitney's U and Kolmogorov-Smirnov tests described in Transparent Methods supplemental file. (H) Unbiased comparative analysis of proteins in two proteomes based on Mascot protein score; 106 proteins were selected by fold change with a cutoff of 5.0. (I) Selected representatives of top-ranked proteins identified in the SBP1 interactomes.

terms for the parasite proteins were predominantly related to proteins exported to host cytoplasm ( $p = 1.6 - 3.5 \times 10^{-4}$ ) (Table S4). The GO analysis further identified enrichment in multiple parasite cellular compartments, including the Sec61 translocon complex (Benjamini-adjusted  $p = 0.0089$ ), rough endoplasmic reticulum (Benjamini-adjusted  $p = 0.014$ ), and nuclear pore (Benjamini-adjusted  $p = 0.024$ ) (Figures 2A and 2B). These results suggest that the identified proteins represent parasite proteins exported to the host cytoplasm, where SBP1 functions to anchor the Maurer's clefts to the host cytoskeleton (Blisnick et al., 2000; Kats et al., 2015) as well as proteins associated with the intracellular trafficking of SBP1 within the parasites.

To verify and validate our findings, we focused on the following 11 proteins: five parasite proteins that interacted with the Maurer's clefts (PIESP2, REX1, REX2, MAHRP1, and MAHRP2), three parasite proteins that have not previously been reported to interact with SBP1 (PF10\_0018, STEVOR, and TryThrA), and three host proteins (STOM, KPNB1, and MPP1). To test whether these proteins interact with endogenous SBP1, we generated parasites expressing FLAG-tagged SBP1 under the control of endogenous promoters by introducing a FLAG tag after the full-length C terminus of SBP1 using single crossover homologous

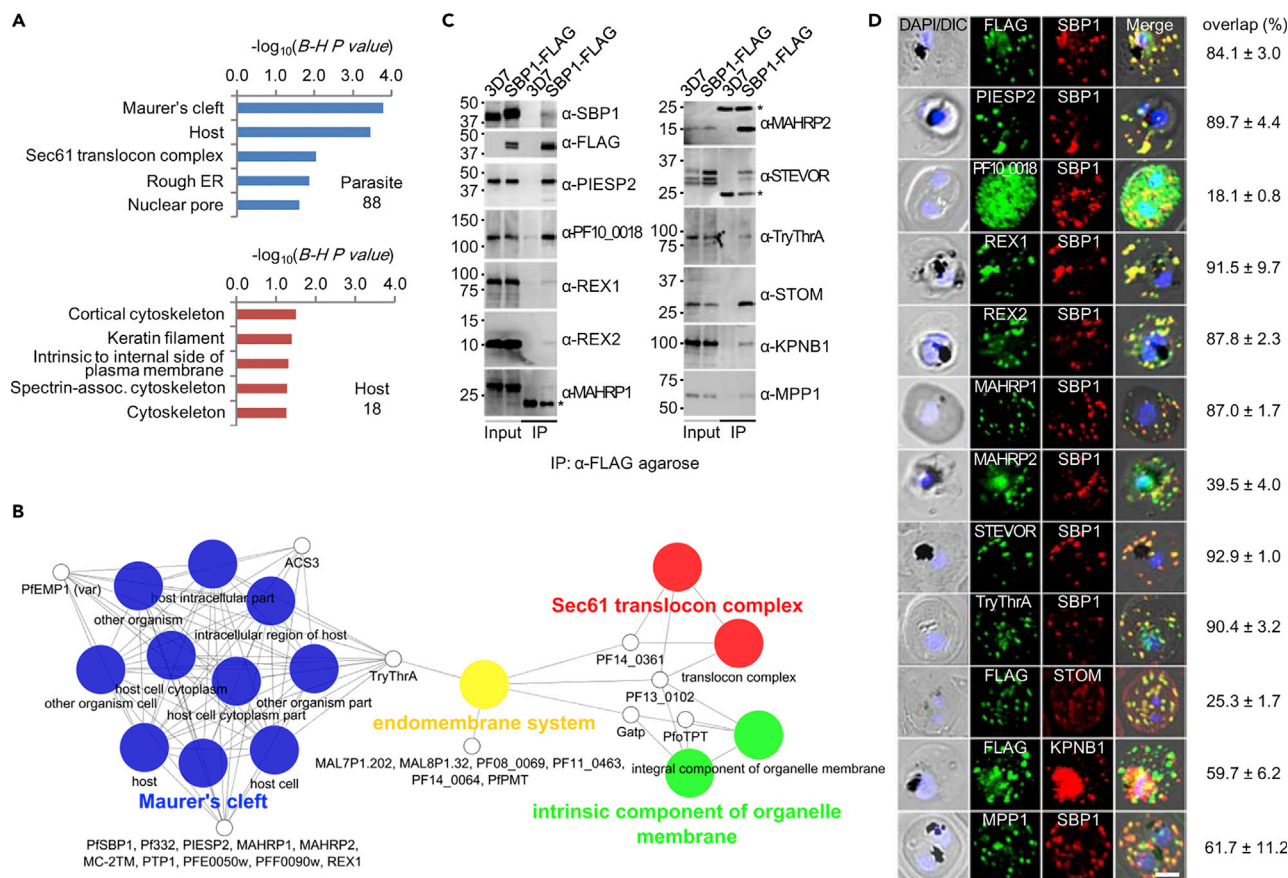


**Figure 2. Verification and Validation of SBP1 Interactomes**

(A) Functional enrichment analyses of likely SBP1-interacting proteins. Gene Ontology analysis was conducted for the parasite (upper panel) and host proteins (lower panel), respectively.

(B) The relationships of the GO terms enriched for the parasite proteins were visualized using Cytoscape with the ClueGO plugin.

(C and D) Biological binding and functional validation of 11 SBP1 interactors by use of co-immunoprecipitation (C) and immunofluorescence (D) assays on endogenous SBP1-FLAG cells. The asterisk indicates a non-specific band that reacted with the light chain of IgG. Scale bar, 3  $\mu$ m. The ratio of co-localization between two factors was analyzed by using Python 3.7.3 and is shown as the mean  $\pm$  SD (n = 10).

recombination (Figure S1). Whole-cell lysates were prepared, and co-immunoprecipitation was carried out as described above. The precipitated proteins were subjected to SDS-PAGE followed by western blot using polyclonal serum from mice immunized with recombinant parasite proteins (details are provided in the Transparent Methods) and commercially available antibodies against the host proteins. We confirmed that all the 11 proteins tested co-immunoprecipitated with endogenous SBP1 by western blot analyses (Figure 2C). Of note, six of the parasite proteins (PIESP2, REX1, REX2, MAHRP1, STEVOR, and TryThrA) co-localized with SBP1 in the Maurer's clefts, whereas the remaining five proteins (two parasite proteins, PF10\_0018 and MAHRP2, and three host proteins, STOM, KPNB1, and MPP1) showed partial co-localization with SBP1 (Figure 2D), presumably reflecting a different role for these proteins in the host cytoplasm; that is, the "full" co-localization proteins may be involved in the trafficking complex in the Maurer's clefts, whereas the "partial" co-localization proteins may be involved in anchoring the Maurer's clefts. Taken together, our unbiased comparative proteomic approach allowed us to systematically identify SBP1-interacting candidates and establish a comprehensive map of SBP1 interactomes in human erythrocytes infected with *P. falciparum*.

### Host-Parasite Interactions Based on SBP1 Interactomes

Our identification of SBP1-interacting candidates sheds light on the complex interplay between multiple parasite proteins and SBP1 throughout the trafficking pathway and highlights plausible parasite-host

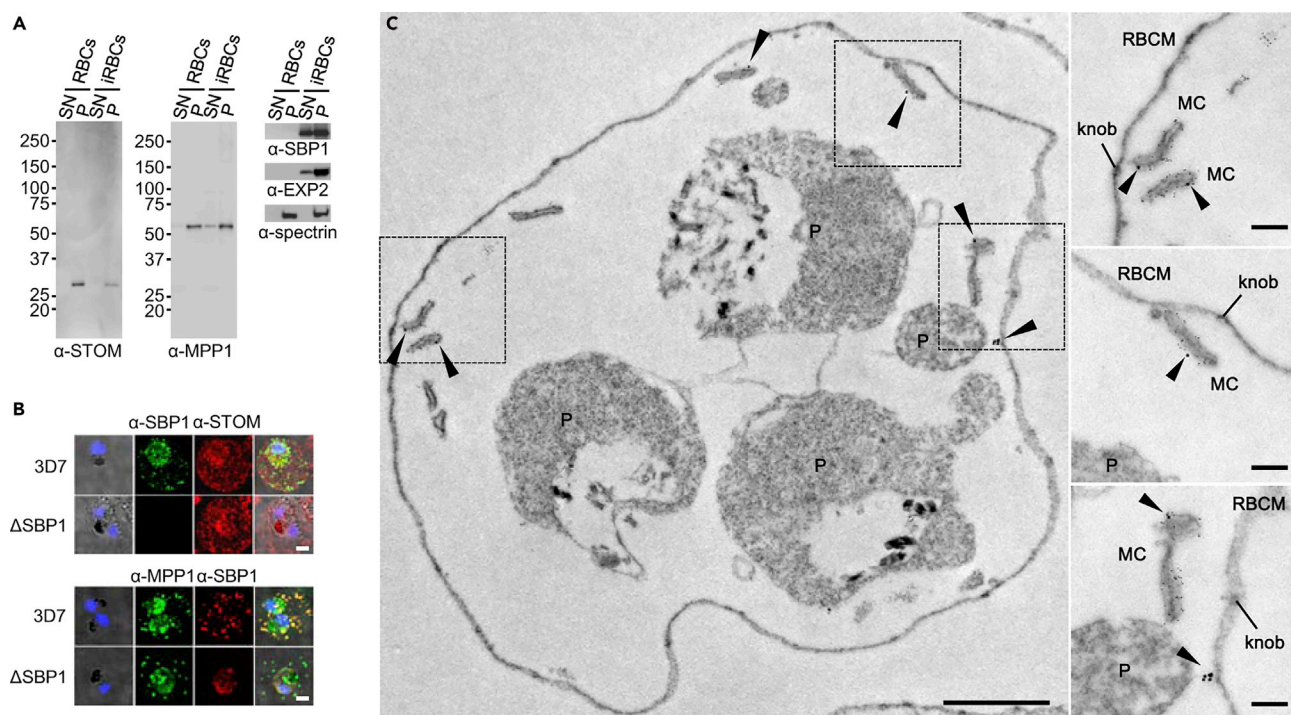


**Figure 3. MPP1 Is Associated with SBP1 in Maurer's Clefts**

(A) Solubility of the host STOM and MPP1 proteins, which interacted with SBP1; uninfected and MACS-purified *P. falciparum* 3D7-infected RBCs (iRBCs) were lysed with 0.09% saponin lysis buffer and equivalent amounts of supernatant and pellet samples were analyzed by western blot.

(B) Immunofluorescence assay of host factors in 3D7/ $\Delta$ SBP1 cells. Scale bar, 2  $\mu$ m.

(C) Double-stained immunoelectron microscopy of tetanolysin-permeabilized iRBCs to confirm MPP1 association with SBP1 in Maurer's clefts. SBP1 and MPP1 were labeled with 5- and 15-nm gold particles, respectively. MPP1 associated with SBP1 in Maurer's clefts apposed to the RBC membrane. MC, Maurer's clefts; P, parasites; RBCM, red blood cell membrane. Scale bars, 1  $\mu$ m and 200 nm, for left and right panels, respectively.

interactions in the host cytoplasm. Of the host proteins that interacted with SBP1, we focused on STOM and MPP1, which are involved in the membrane organization of erythrocytes (Biernatowska et al., 2017; Lach et al., 2012; Salzer and Prohaska, 2001). To determine whether these proteins are associated with the erythrocyte cytoskeleton, we examined their solubility (Figure 3A). Solubility assays revealed that STOM remained exclusively in the pellet corresponding to membrane ghost fractions (similar to spectrin), whereas a portion of MPP1 was released into the detergent-sensitive supernatant fractions, suggesting the presence of soluble MPP1 in the host cytoplasm, consistent with previous studies (Biernatowska et al., 2017; Lach et al., 2012).

To examine the effects of SBP1 on the localization of these two host proteins, we next generated SBP1-deficient transgenic parasites (Cooke et al., 2006; Maier et al., 2007) and analyzed the protein localization in erythrocytes infected with wild-type or  $\Delta$ SBP1 parasites (Figure 3B). The absence of SBP1 did not influence the localization of these two proteins; the MPP1 signal was detected in the Maurer's clefts and infected RBC (iRBC) membrane regardless of whether SBP1 was present. To further examine whether MPP1 associates with SBP1 in Maurer's clefts, we performed immunoelectron microscopy using gold particle co-labeling of MPP1 and SBP1 (Figure 3C). We observed that MPP1 was closely associated with SBP1 in the Maurer's clefts, but that a portion of MPP1 was detectable just beneath the erythrocyte membrane where the SBP1 signal was not detected (Figure 3C). Thus, we identified the host protein MPP1 as being recruited into Maurer's clefts, suggesting that it may play a role in the membrane organization of these clefts.

### Using SBP1 Interactomes to Reveal the Exportome

Previous proteomic studies of the protein components of the trafficking complex (Batinovic et al., 2017; Rug et al., 2014) and of secreted microvesicles (Mantel et al., 2013) identified a limited number of exported proteins (Figure S2). Our SBP1 interactomes highly enrich our knowledge of the known exported proteins

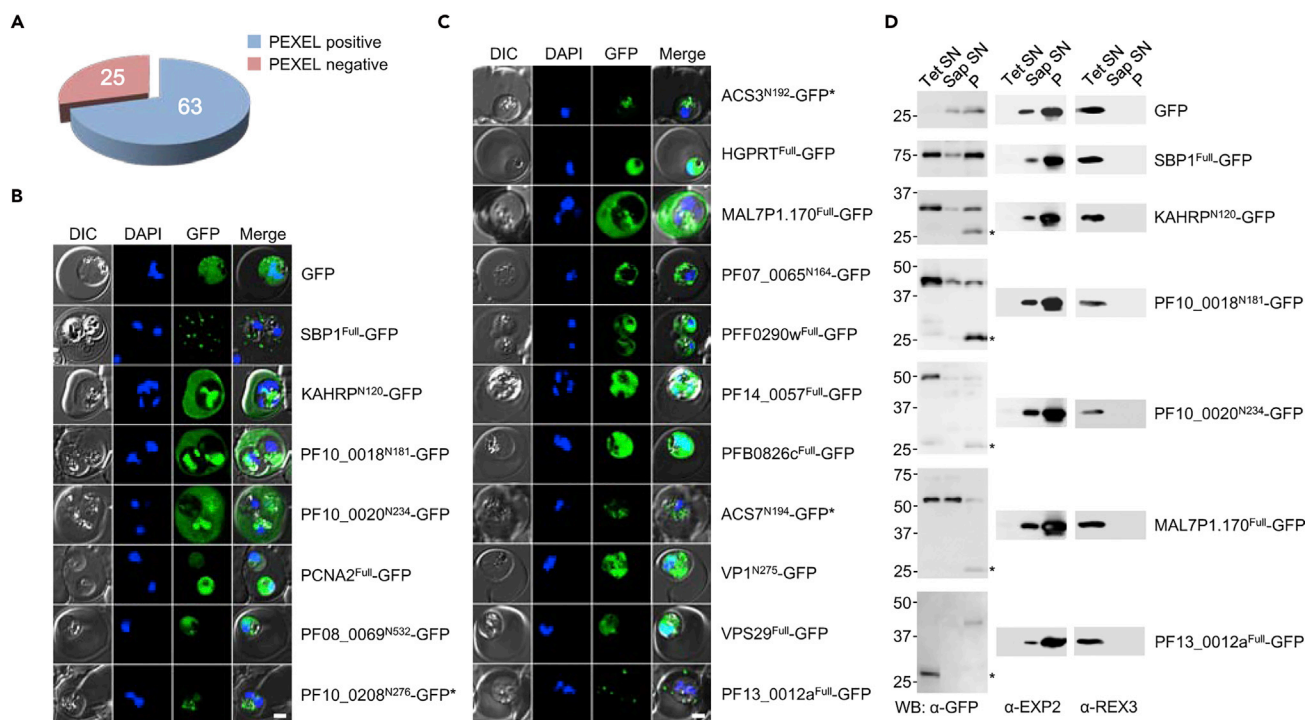


**Figure 4. GFP-Based Protein Export Assay Identifies Four Exported Proteins**

(A) Abundance of proteins with a PEXEL sequence [(R/K)xLx(D/E/Q)] among 88 parasite factors that interacted with SBP1.

(B and C) Live-cell images of parasites expressing the N terminus or full-length of 5 PEXEL (B) and 11 non-PEXEL (C) proteins fused with GFP. GFP alone and GFP-fused SBP1 and KAHRP are shown as controls. Nuclei are stained with DAPI. Scale bar, 2  $\mu$ m. The expression of GFP fusion proteins for the cell lines tested is shown in Figure S3A. The results of immunofluorescence assays using anti-GFP antibodies on three mutants showing weak GFP fluorescence (indicated by the asterisk) are shown in Figure S3B.

(D) Western blot analyses using anti-GFP with extracts from selective permeabilization assays show bands with full-length or truncated versions of four exported GFP fusion proteins. SN, supernatants; Tet, tetanolysin (host cytosol); Sap, saponin (Maurer's clefts and parasitophorous vacuoles); P, pellet (final pellet); REX3, soluble parasite proteins in host cells; EXP2, parasitophorous vacuole marker. Asterisk, degradation product.

identified in previous proteomic studies (Figure S2) and reveal a previously unknown association between a host protein, MPP1, and the Maurer's clefts.

Among the 88 parasite proteins identified in our SBP1 interactomes, we found 63 proteins with the canonical PEXEL motif [(R/K)xLx(D/E/Q)], which is present in many exported proteins (Figure 4A). We focused on the following 16 proteins: 5 proteins with the PEXEL motif (PF10\_0018, PF10\_0020, PCNA2, PF08\_0069, and PF10\_0208) and 11 proteins lacking the PEXEL motif (ACS3, HGPRT, MAL7P1.170, PF07\_0065, PFF0290w, PF14\_0057, PFB0826c, ACS7, VP1, VPS29, and PF13\_0012a), and re-examined their intracellular localization.

To test whether these proteins are exported into the host cytoplasm, we conducted a GFP-based protein export assay as established previously (Dixon et al., 2008; Heiber et al., 2013; Spielmann et al., 2006). The full length or N terminus of each candidate was C-terminally tagged with GFP and expressed episomally in *P. falciparum*. In parallel, GFP alone and GFP-tagged SBP1 and KAHRP were expressed and used as controls. The expression of the GFP-fused proteins of each mutant was confirmed by western blot (Figure S3A). Of the mutant cell lines tested, three showed weak GFP fluorescence (PF10\_0208, ACS3, and ACS7), nine showed no evidence of export (PCNA2, PF08\_0069, HGPRT, PF07\_0065, PFF0290w, PF14\_0057, PFB0826c, VP1, and VPS29), and four showed export (PF10\_0018, PF10\_0020, MAL7P1.170, and PF13\_0012a) (Figures 4B and 4C). For the three mutants showing weak GFP fluorescence, we performed immunofluorescence staining using an  $\alpha$ -GFP antibody and showed no evidence of export (Figure S3B). Of the four exported proteins, PF10\_0018-GFP, PF10\_0020-GFP, and MAL7P1.170-GFP were distributed throughout the host cytoplasm, whereas PF13\_0012a-GFP produced characteristic fluorescence in the Maurer's clefts.

To define the subcellular localization of the four exported proteins, we conducted a selective permeabilization assay on erythrocytes infected with each mutant parasite (Boddey et al., 2016; Gruring et al., 2012; Mantel et al., 2016) (Figure 4D). Sequential treatment of iRBCs with tetanolysin and saponin separates the cells into RBC cytosol, a parasitophorous vacuole and Maurer's clefts, a parasite membrane fraction, and a host membrane fraction (Mantel et al., 2016). Western blot analyses demonstrated that all four exported proteins were present in the soluble fractions representing RBC cytosol, thereby confirming the observed localization of these proteins in the live-cell imaging analyses (Figure 4D). Thus the SBP1 interactomes established by our alternative proteomic approaches led us to discover four exported proteins regardless of whether they contained the PEXEL motif.

### Necessity and Significance of SBP1-Interacting Proteins

In light of the functional importance of SBP1 for the host cell remodeling that is required for malaria virulence, we asked whether disruption of genes encoding SBP1 interactors could affect malaria survival and pathogenesis. To concentrate on genes that encoded exported proteins for knockout experiments, we first curated a list of genes by selecting those specifically expressed during the ring stage from Table S2, as well as the top-ranked 25 hit genes from Table S3, resulting in a set of 37 genes. This set contained seven genes that encode well-known exported proteins required for malaria virulence (*SBP1*, *MAHRP1*, *MAHRP2*, *REX1*, *REX2*, *PTP1*, and *PTP5*) (Figure S4). We therefore focused on 13 SBP1-interacting genes (*PF10\_0018*, *ACS3*, *PF13\_0309*, *PF08\_0069*, *vapA*, *FIKK10.2*, *TryThrA*, *ACS7*, *VP1*, *STARP*, *PFL2530w*, *PF14\_0045*, and *MAL8P1.4*) whose functions remain to be fully elucidated, plus *SBP1*, and performed targeted gene disruption experiments by using the double homologous recombination system described previously (Maier et al., 2008) (Figures S5 and S6).

Of 14 genes tested, seven (*SBP1*, *PF10\_0018*, *FIKK10.2*, *TryThrA*, *STARP*, *PFL2530w*, and *MAL8P1.4*) could be genetically disrupted, suggesting that the other seven genes are essential to the parasite during the asexual blood stage (Figures 5A and S4–S6). Of the seven genes that were disrupted, six encode exported proteins (*SBP1*, *PF10\_0018*, *FIKK10.2*, *TryThrA*, *STARP*, and *MAL8P1.4*), which is consistent with previous findings that genes encoding exported proteins are less essential for parasite asexual development than those encoding non-exported proteins (Bushell et al., 2017; Maier et al., 2008). We did not see any substantial differences in parasite growth or invasion between the wild-type parasite and each knockout mutant (Figures S7A and S7B). These results suggest that the exported proteins encoded by these six genes may play roles in host cell remodeling by interacting with SBP1.

We then focused on three knockout cell lines ( $\Delta$ *TryThrA*,  $\Delta$ *STARP*, and  $\Delta$ *MAL8P1.4*), in which genes that encoded proteins located in Maurer's clefts were disrupted, and tested their cytoadherence by using a CD36 static binding assay. We found that  $\Delta$ *TryThrA* and  $\Delta$ *STARP* showed comparable levels of cytoadherence relative to those of the wild-type, whereas disruption of the *MAL8P1.4* gene resulted in increased cytoadherence of iRBCs to CD36 (Figure 5B). Intriguingly, we did not observe any changes in the localization of known exported proteins, represented by SBP1, PfEMP1, MAHRP1, and REX1, or any alternations in knob formation or Maurer's cleft morphology in the erythrocytes infected with  $\Delta$ *MAL8P1.4* parasites compared with those in the erythrocytes infected with wild-type parasites (Figures S7C–S7G). Thus, by performing gene knockout experiments followed by cytoadherence assays on 14 genes that encode potential SBP1 interactors, we identified *MAL8P1.4* as being associated with the cytoadherence of iRBCs and thereby affecting malaria virulence.

### DISCUSSION

Here, we developed an authentic, unbiased, and highly sensitive comparative proteomic approach to characterize proteins that interact with SBP1. This approach allowed us to identify more than 100 putative proteins, which were enriched with known exported proteins that play central roles in host cell remodeling. On the basis of SBP1 interactomes, we further conducted systematic analyses to validate the factors that were associated with SBP1 in the cytoplasm of erythrocytes (Figure 5C) and identified a parasite protein, *MAL8P1.4*, which regulates the cytoadherence of *P. falciparum*-infected erythrocytes to vascular endothelial receptors.

Regarding the quality of the interactome we have presented, it must be noted that we cannot exclude the possibility that our dataset contains false-positives. However, by performing validation studies on previously known and unknown SBP1-interacting proteins, we have been able to show that our SBP1 interactomes are reliable and invaluable for the clarification of the exportome. This significantly increases the

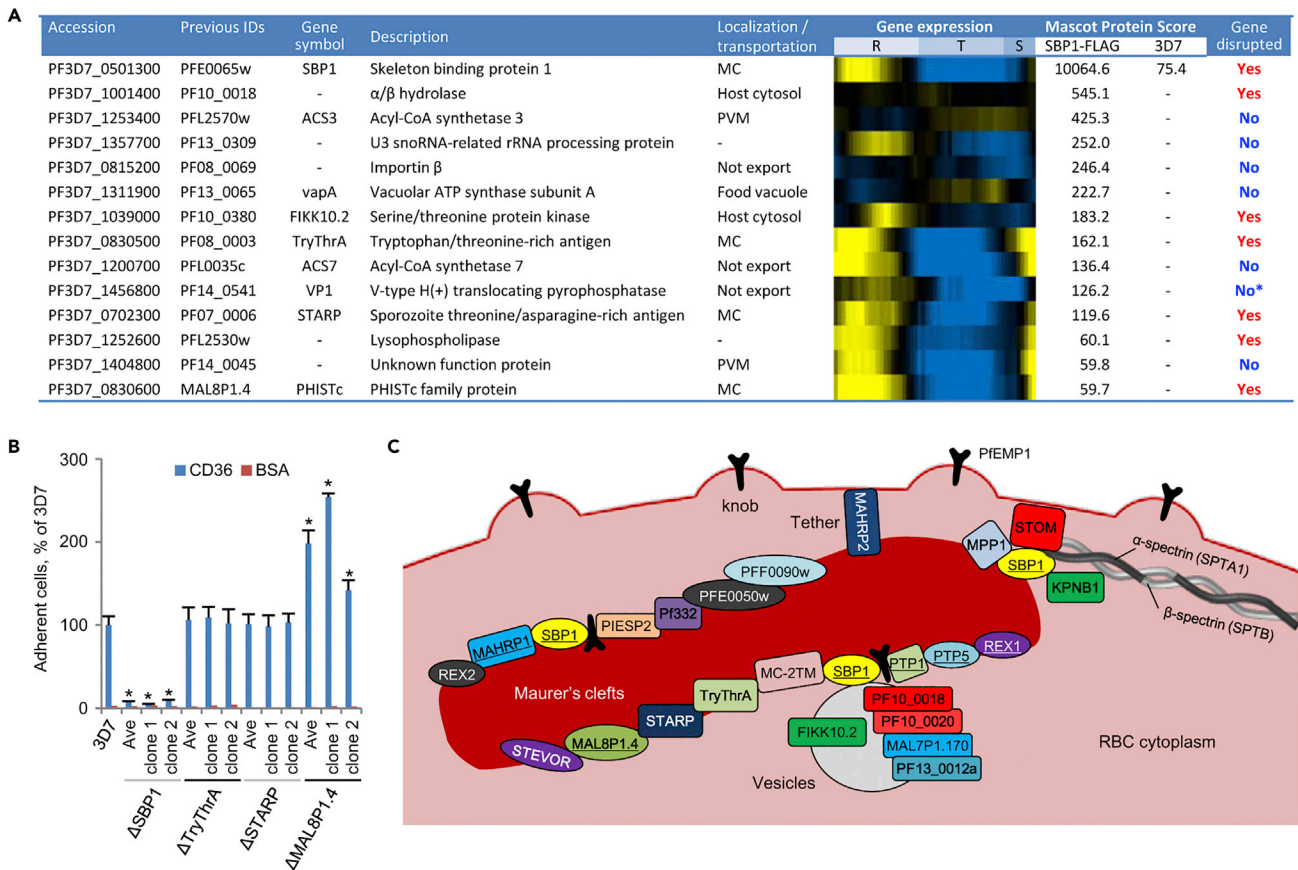


**Figure 5. Necessity and Significance of SBP1 Interactors for Parasites in the Asexual Blood Stage**

(A) Genes selected for knockout studies. Shown in the first to fourth columns are the accession number, previous ID, gene symbol, and gene description from PlasmoDB (<http://www.plasmo.org>). The fifth column shows the subcellular localization of the protein in the infected erythrocyte if known and whether or not the protein is exported based on the results of the protein export assay shown in Figure 4. The sixth column shows a transcriptional profile where yellow denotes an increased period of transcription and blue denotes a decreased period or no transcription. Gene expression data were obtained from the DeRisi's microarray data available in PlasmoDB. R, ring; T, trophozoite; S, schizont asexual life cycle stages. The seventh column shows the Protein Mascot Score of each protein in the SBP1-FLAG/3D7 proteomes; - denotes not detected. The eighth column refers to whether the gene can be genetically disrupted (Yes) or not (No). Asterisk, undetermined because of delayed growth of parasites transfected with gene-targeting plasmid.

(B) Adherence of mutant parasite-infected erythrocytes to CD36 receptors under static conditions. Two clones of each mutant parasite were tested for binding to CD36 receptors; adherent cells were counted and are shown as a ratio relative to the level of 3D7-infected erythrocytes. The values presented are the average of three independent experiments  $\pm$  SD. *P* values were calculated by using one-way ANOVA with Tukey's post-hoc test ( $*P < 0.05$ ).

(C) Overview of the protein-protein interactions uncovered by our SBP1 interactomes. Three host proteins (STOM, KPNB1, and MPP1), two parasite proteins (PF10\_0018, and PF10\_0020), and six parasite exported proteins (STEVOR, PF332, TryThrA, STARP, PF13\_0012a, and MAL8P1.4) identified in our study are shown in boldface. Proteins involved in cytoadherence are underlined.

value of our dataset as a resource because the entire dataset used for our analyses is presented here and can be analyzed independently. It is also important to note that our established system to identify SBP1-interacting proteins is completely authentic and unbiased regarding protein identification. Because of technical difficulties using co-immunoprecipitation to study protein-protein interactions in the cytoplasm of erythrocytes infected with parasites, most previous interactome studies (Batinovic et al., 2017; Dietz et al., 2014; Oberli et al., 2016) have been done on parasite lysates after saponin lysis to remove the host cell cytosol, Maurer's clefts, and soluble parasitophorous vacuole contents. This is because erythrocytes contain abundant cytoskeleton proteins, which easily and non-specifically bind to beads, leading to loss of important information regarding protein interactions in the host cytoplasm. To overcome these difficulties, we carried out co-immunoprecipitation experiments on whole-cell lysates of purified iRBCs, analyzed the precipitated proteins by using shotgun proteomics, and performed quantitative analyses of the two proteomes obtained. The dataset derived by taking this approach includes many of the exported proteins previously characterized. In fact, our proteomic data covered 16 of the known exported proteins

(PfEMP1, FIKK10.1, PTP1, PFF0090w, PFA0210c, GEXP10, SBP1, PIESP2, REX1, MAHRP1, MAHRP2, Pf332, REX2, PFE0050w, GEXP07, and MC-2TM) of the 21 overlapping proteins identified in three previous proteomic studies (Batinovic et al., 2017; Mantel et al., 2013; Rug et al., 2014). Our study further confirmed that these proteins made authentic interactions in the host cytoplasm (Figure S2). With these advantages, our SBP1 interactomes could serve as intermediaries to connect previous studies (Batinovic et al., 2017; Dietz et al., 2014; Mantel et al., 2013; Oberli et al., 2016; Rug et al., 2014) of exported proteins. The application of our proteomic approaches to other exported proteins resident in Maurer's clefts would greatly increase our understanding of the interaction network of the *P. falciparum* exportome.

Recently, the *P. falciparum* orthologs of SBP1 and MAHRP1 were discovered in the rodent malaria *Plasmodium berghei* by De Niz et al. (De Niz et al., 2016), and disruption of these genes resulted in the decreased cytoadherence of iRBCs to CD36 in a mouse model, suggesting that these genes are likely involved in the transport of an unidentified parasite ligand that allows binding of iRBCs to vascular endothelium, similar to *P. falciparum* SBP1 and MAHRP1 (Cooke et al., 2006; Maier et al., 2007; Spycher et al., 2008). Given that our proteomic studies identified a solid interaction between SBP1 and PfEMP1, our approach could be used to identify such unidentified parasite ligands of rodent malaria.

Our analyses led us to identify three parasite proteins (PF10\_0018, STEVOR, and TryThrA) associated with the trafficking complex, as well as several host-parasite protein interactions (STOM, KPNB1, and MPP1). PF10\_0018 was identified as a highly ranked SBP1 interactor, and its homolog PF10\_0020 was also identified with a high probability-based score in our proteomic analyses (see Tables S2 and S3). These two genes encode proteins that belong to the  $\alpha/\beta$  hydrolase family, have the highest sequence similarity in our study (Figure S8), and were recently shown to be efficiently exported (Spillman et al., 2016). However, their roles in the host cytoplasm remain completely unknown. Given the predicted lysophospholipase activity of PF10\_0018 and PF10\_0020, and that a variety of pathogens exploit host lipids to modify their membrane compositions (van der Meer-Janssen et al., 2010), these proteins might play a role in the lipid metabolism required for the generation of Maurer's clefts.

A tryptophan-threonine-rich antigen (termed by TryThrA) was also identified as a parasite protein associated with SBP1 in the trafficking complex. TryThrA was previously characterized as a protein expressed on merozoite surface and involved in parasite invasion, which is supported by the inhibitory effect of synthetic peptides of TryThrA antigen on merozoite invasion of erythrocytes (Curtidor et al., 2006). In the current study, we found that TryThrA was expressed across the asexual cycle and localized in Maurer's clefts (See Figure S9). Moreover, we demonstrated that its gene could be genetically disrupted without affecting parasite invasion (Figure S7B), which is inconsistent with previous studies (Alam et al., 2015; Curtidor et al., 2006). This discrepancy could be explained by off-target effects of the synthetic peptides used in the previous studies, or by alternative expression of molecules that could compensate for the loss of TryThrA in our knockout parasites. Further studies are warranted to elucidate the precise function of TryThrA in infected erythrocytes.

Host-parasite protein interactions play an essential role in malaria progression and pathogenesis (Egan et al., 2015; Miller et al., 2002; Olszewski et al., 2009). Here, we identified several host-parasite protein interactions in the host cytoplasm. Of three host factors identified (STOM, KPNB1, and MPP1), we found that MPP1, membrane palmitoylated protein 1 (also termed p55, 55 kDa erythrocyte membrane protein), was recruited into the Maurer's clefts (Figure 3C). MPP1 is a member of the membrane-associated guanylate kinase (MAGUK) family and plays essential roles in membrane organization of erythroid cells, composition of lipid rafts on erythrocyte membranes, and erythrocytopoiesis (Biernatowska et al., 2017; Egan et al., 2015; Lach et al., 2012; Quinn et al., 2009). Moreover, a previous proteomic study of microvesicles, which are secreted from the surface of *P. falciparum*-infected erythrocytes and likely bud from Maurer's clefts (Mantel et al., 2013), identified the presence of this protein. These results suggest that MPP1 might contribute to the organization of the membranous structures of Maurer's clefts.

Our series of knockout experiments followed by cytoadherence assays on potential SBP1 interactors identified MAL8P1.4 as being involved in the cytoadherence of iRBCs to vascular endothelial receptors (Figure 5B). MAL8P1.4 is a member of the *Plasmodium* helical interspersed subtelomeric (*PHIST*) family of exported proteins, which play diverse roles in parasite-infected erythrocytes (Kumar et al., 2018; Oberli et al., 2014, 2016; Proellocks et al., 2014). Although the function of *PHIST* genes remains to be fully elucidated,

previous studies have revealed that specific PHIST proteins can bind to the acidic C-terminal (ATS) domain of PfEMP1 and that depletion of genes that encode PHIST proteins results in decreased cytoadherence (Oberli et al., 2016; Proellocks et al., 2014). Moreover, the binding capacity of a PHIST protein differs for each PfEMP1 depending on the sequence of its ATS domain (Kumar et al., 2018; Oberli et al., 2016), suggesting that *PHIST* genes might have coevolved with specific ATS domains to create interaction pairs with maximum binding strength to transport a specific PfEMP1 to the erythrocyte membrane (Kumar et al., 2018; Oberli et al., 2014; Proellocks et al., 2014). In contrast, it has also been reported that MAL8P1.4 does not localize to the surface of erythrocytes or a knob and has low binding affinity for an ATS domain of a specific PfEMP1 (Oberli et al., 2014). Although there are many unknowns regarding the function of MAL8P1.4, given that multiple PHIST proteins are cooperatively and selectively involved in the transport of a specific PfEMP1 to the erythrocyte surface (Oberli et al., 2016), the altered cytoadherence by  $\Delta$ MAL8P1.4 parasites may arise from the alternation of PfEMP1 being transported and presented on the erythrocyte surface. Further investigations of the relationships between cognate genes, in addition to a genetic complementation study of the MAL8P1.4 gene, would reveal the mechanistic details of the cytoadherence required for malaria virulence.

In summary, we present a comprehensive map of SBP1 interactomes to better understand the intraerythrocytic trafficking complex and interactions between host and parasite proteins in the host cytoplasm. We used this information to identify exported proteins required for cytoadherence of *P. falciparum*-infected erythrocytes and found that disruption of *MAL8P1.4* resulted in altered cytoadherence of iRBCs to endothelial receptors with no appreciable effects on parasite viability or host cell remodeling. These findings demonstrate that our original approach using unbiased comparative shotgun proteomics provides significant insights into the complicated interplay between host and parasite proteins in the trafficking complex and creates pathways to study the molecular basis of the virulence of *P. falciparum*-infected erythrocytes.

### Limitation of the Study

The present study led us to identify multiple host- and parasite-derived proteins that interact with SBP1, but it did not lead to the detailed function elucidation of the identified factors. Detailed analyses of how MPP1 or MAL8P1.4 is involved in the formation and configuration of Maurer's clefts, as well as cell adhesion, are needed. Moreover, to determine whether our results are universally applicable, further studies using different *P. falciparum* strains should be done.

### METHODS

All methods can be found in the accompanying [Transparent Methods supplemental file](#).

### SUPPLEMENTAL INFORMATION

Supplemental Information can be found online at <https://doi.org/10.1016/j.isci.2019.07.035>.

### ACKNOWLEDGMENTS

We thank Susan Watson for editing the manuscript. We thank Dr. Takafumi Tsuboi (Ehime University, Japan) for providing rabbit anti-EXP2 and mouse and rabbit anti-SBP1 antibodies, and Dr. Alan F. Cowman (Walter Eliza Hall Institute for Medical Research, Australia) for the pARL1 transfection plasmid. We also thank Drs. Hitoshi Takemae, Tatsuki Sugi, and Takeshi Q. Tanaka (Obihiro University of Agriculture and Veterinary Medicine, Japan) and Dr. Motomi Torii (Ehime University, Japan) for technical advice and useful discussions. This work was supported by Grants-in-Aid for Young Scientists and Scientific Research on Innovative Areas (3308) from the Ministry of Education, Culture, Science, Sports, and Technology (MEXT) of Japan, the Program to Disseminate Tenure Tracking System from the Japan Science and Technology Agency (JST), the Takeda Science Foundation, and the Suhara Memorial Foundation.

R.T. is supported by Research Fellowships from the Japan Society for the Promotion of Science for Young Scientists from the MEXT of Japan.

### AUTHOR CONTRIBUTIONS

R.T. conceived and designed the project, performed the experiments, analyzed the data, and prepared and wrote the manuscript. H.K.-H., and M.O. performed the mass spectrometry analyses. D.K. and H.B.

performed the electron microscopic analyses. K.K. supervised and oversaw the project. All authors approved the final manuscript.

## DECLARATION OF INTERESTS

The authors declare that no competing interests exist.

Received: December 17, 2018

Revised: May 9, 2019

Accepted: July 19, 2019

Published: September 27, 2019

## REFERENCES

- Alam, M.S., Choudhary, V., Zeeshan, M., Tyagi, R.K., Rathore, S., and Sharma, Y.D. (2015). Interaction of *Plasmodium vivax* tryptophan-rich antigen PvTRAg38 with band 3 on human erythrocyte surface facilitates parasite growth. *J. Biol. Chem.* *290*, 20257–20272.
- Batinovic, S., McHugh, E., Chisholm, S.A., Matthews, K., Liu, B., Dumont, L., Charnaud, S.C., Schneider, M.P., Gilson, P.R., de Koning-Ward, T.F., et al. (2017). An exported protein-interacting complex involved in the trafficking of virulence determinants in *Plasmodium*-infected erythrocytes. *Nat. Commun.* *8*, 16044.
- Biernatowska, A., Augoff, K., Podkalicka, J., Tabaczar, S., Gajdzik-Nowak, W., Czogalla, A., and Sikorski, A.F. (2017). MPP1 directly interacts with flotillins in erythrocyte membrane - Possible mechanism of raft domain formation. *Biochim. Biophys. Acta Biomembr.* *1859*, 2203–2212.
- Blisnick, T., Morales Betoulle, M.E., Barale, J.C., Uzureau, P., Berry, L., Desroses, S., Fujioka, H., Mattei, D., and Braun Breton, C. (2000). Pfsbp1, a Maurer's cleft *Plasmodium falciparum* protein, is associated with the erythrocyte skeleton. *Mol. Biochem. Parasitol.* *111*, 107–121.
- Boddey, J.A., O'Neill, M.T., Lopaticki, S., Carvalho, T.G., Hodder, A.N., Nebli, T., Wawra, S., van West, P., Ebrahimzadeh, Z., Richard, D., et al. (2016). Export of malaria proteins requires co-translational processing of the PEXEL motif independent of phosphatidylinositol-3-phosphate binding. *Nat. Commun.* *7*, 10470.
- Bushell, E., Gomes, A.R., Sanderson, T., Anar, B., Girling, G., Herd, C., Metcalf, T., Modrzynska, K., Schwach, F., Martin, R.E., et al. (2017). Functional profiling of a plasmodium genome reveals an abundance of essential genes. *Cell* *170*, 260–272.e8.
- Cooke, B.M., Buckingham, D.W., Glenister, F.K., Fernandez, K.M., Bannister, L.H., Marti, M., Mohandas, N., and Coppel, R.L. (2006). A Maurer's cleft-associated protein is essential for expression of the major malaria virulence antigen on the surface of infected red blood cells. *J. Cell Biol.* *172*, 899–908.
- Curtidor, H., Ocampo, M., Rodriguez, L.E., Lopez, R., Garcia, J.E., Valbuena, J., Vera, R., Puentes, A., Leiton, J., Cortes, L.J., et al. (2006). *Plasmodium falciparum* TryThrA antigen synthetic peptides block in vitro merozoite invasion to erythrocytes. *Biochem. Biophys. Res. Commun.* *339*, 888–896.
- De Niz, M., Ullrich, A.K., Heiber, A., Blancke Soares, A., Pick, C., Lyck, R., Keller, D., Kaiser, G., Prado, M., Flemming, S., et al. (2016). The machinery underlying malaria parasite virulence is conserved between rodent and human malaria parasites. *Nat. Commun.* *7*, 11659.
- Dietz, O., Rusch, S., Brand, F., Mundwiler-Pachlatko, E., Gaida, A., Voss, T., and Beck, H.P. (2014). Characterization of the small exported *Plasmodium falciparum* membrane protein SEMP1. *PLoS One* *9*, e103272.
- Dixon, M.W., Hawthorne, P.L., Spielmann, T., Anderson, K.L., Trenholme, K.R., and Gardiner, D.L. (2008). Targeting of the ring exported protein 1 to the Maurer's clefts is mediated by a two-phase process. *Traffic* *9*, 1316–1326.
- Egan, E.S., Jiang, R.H., Moehtar, M.A., Barteneva, N.S., Weekes, M.P., Nobre, L.V., Gygi, S.P., Paulo, J.A., Frantzeb, C., Tani, Y., et al. (2015). Malaria. A forward genetic screen identifies erythrocyte CD55 as essential for *Plasmodium falciparum* invasion. *Science* *348*, 711–714.
- Fairhurst, R.M., Baruch, D.I., Brittain, N.J., Ostera, G.R., Wallach, J.S., Hoang, H.L., Hayton, K., Guindo, A., Makobongo, M.O., Schwartz, O.M., et al. (2005). Abnormal display of PfEMP-1 on erythrocytes carrying haemoglobin C may protect against malaria. *Nature* *435*, 1117–1121.
- Gorai, T., Goto, H., Noda, T., Watanabe, T., Kozuka-Hata, H., Oyama, M., Takano, R., Neumann, G., Watanabe, S., and Kawaoka, Y. (2012). F1Fo-ATPase, F-type proton-translocating ATPase, at the plasma membrane is critical for efficient influenza virus budding. *Proc. Natl. Acad. Sci. U S A* *109*, 4615–4620.
- Gruring, C., Heiber, A., Kruse, F., Flemming, S., Franci, G., Colombo, S.F., Fasana, E., Schoeler, H., Borgese, N., Stunnenberg, H.G., et al. (2012). Uncovering common principles in protein export of malaria parasites. *Cell Host Microbe* *12*, 717–729.
- Hanssen, E., Hawthorne, P., Dixon, M.W., Trenholme, K.R., McMillan, P.J., Spielmann, T., Gardiner, D.L., and Tilley, L. (2008). Targeted mutagenesis of the ring-exported protein-1 of *Plasmodium falciparum* disrupts the architecture of Maurer's cleft organelles. *Mol. Microbiol.* *69*, 938–953.
- Heiber, A., Kruse, F., Pick, C., Gruring, C., Flemming, S., Oberli, A., Schoeler, H., Retzlaff, S., Mesen-Ramirez, P., Hiss, J.A., et al. (2013). Identification of new PNEPs indicates a substantial non-PEXEL exportome and underpins common features in *Plasmodium falciparum* protein export. *PLoS Pathog.* *9*, e1003546.
- Hiller, N.L., Bhattacharjee, S., van Ooij, C., Liolios, K., Harrison, T., Lopez-Estrano, C., and Haldar, K. (2004). A host-targeting signal in virulence proteins reveals a secretome in malarial infection. *Science* *306*, 1934–1937.
- Janes, J.H., Wang, C.P., Levin-Edens, E., Vigan-Womas, I., Guillotte, M., Melcher, M., Mercereau-Puijalon, O., and Smith, J.D. (2011). Investigating the host binding signature on the *Plasmodium falciparum* PfEMP1 protein family. *PLoS Pathog.* *7*, e1002032.
- Kats, L.M., Proellocks, N.I., Buckingham, D.W., Blanc, L., Hale, J., Guo, X., Pei, X., Herrmann, S., Hanssen, E.G., Coppel, R.L., et al. (2015). Interactions between *Plasmodium falciparum* skeleton-binding protein 1 and the membrane skeleton of malaria-infected red blood cells. *Biochim. Biophys. Acta* *1848*, 1619–1628.
- Kumar, V., Kaur, J., Singh, A.P., Singh, V., Bisht, A., Panda, J.J., Mishra, P.C., and Hora, R. (2018). PHISTC protein family members localize to different subcellular organelles and bind *Plasmodium falciparum* major virulence factor PfEMP-1. *FEBS J.* *285*, 294–312.
- Lach, A., Grzybek, M., Heger, E., Korycka, J., Wolny, M., Kubiak, J., Kolondra, A., Boguslawski, D.M., Augoff, K., Majkowski, M., et al. (2012). Palmitoylation of MPP1 (membrane-palmitoylated protein 1)/p55 is crucial for lateral membrane organization in erythroid cells. *J. Biol. Chem.* *287*, 18974–18984.
- LaCount, D.J., Vignali, M., Chettier, R., Phansalkar, A., Bell, R., Hesselberth, J.R., Schoenfeld, L.W., Ota, I., Sahasrabudhe, S., Kurschner, C., et al. (2005). A protein interaction network of the malaria parasite *Plasmodium falciparum*. *Nature* *438*, 103–107.
- Lanzer, M., Wickert, H., Krohne, G., Vincensini, L., and Braun Breton, C. (2006). Maurer's clefts: a novel multi-functional organelle in the cytoplasm of *Plasmodium falciparum*-infected erythrocytes. *Int. J. Parasitol.* *36*, 23–36.
- Maier, A.G., Cooke, B.M., Cowman, A.F., and Tilley, L. (2009). Malaria parasite proteins that remodel the host erythrocyte. *Nat. Rev. Microbiol.* *7*, 341–354.

- Maier, A.G., Rug, M., O'Neill, M.T., Beeson, J.G., Marti, M., Reeder, J., and Cowman, A.F. (2007). Skeleton-binding protein 1 functions at the parasitophorous vacuole membrane to traffic PfEMP1 to the *Plasmodium falciparum*-infected erythrocyte surface. *Blood* 109, 1289–1297.
- Maier, A.G., Rug, M., O'Neill, M.T., Brown, M., Chakravorty, S., Szeszak, T., Chesson, J., Wu, Y., Hughes, K., Coppel, R.L., et al. (2008). Exported proteins required for virulence and rigidity of *Plasmodium falciparum*-infected human erythrocytes. *Cell* 134, 48–61.
- Mantel, P.Y., Hjelmqvist, D., Walch, M., Kharoubi-Hess, S., Nilsson, S., Ravel, D., Ribeiro, M., Gruring, C., Ma, S., Padmanabhan, P., et al. (2016). Infected erythrocyte-derived extracellular vesicles alter vascular function via regulatory Ago2-miRNA complexes in malaria. *Nat. Commun.* 7, 12727.
- Mantel, P.Y., Hoang, A.N., Goldowitz, I., Potashnikova, D., Hamza, B., Vorobjev, I., Ghiran, I., Toner, M., Irimia, D., Ivanov, A.R., et al. (2013). Malaria-infected erythrocyte-derived microvesicles mediate cellular communication within the parasite population and with the host immune system. *Cell Host Microbe* 13, 521–534.
- Marti, M., Good, R.T., Rug, M., Knuepfer, E., and Cowman, A.F. (2004). Targeting malaria virulence and remodeling proteins to the host erythrocyte. *Science* 306, 1930–1933.
- Mbengue, A., Vialla, E., Berry, L., Fall, G., Audiger, N., Demetree-Verceil, E., Boteller, D., and Braun-Breton, C. (2015). New export pathway in *Plasmodium falciparum*-infected erythrocytes: role of the parasite group II chaperonin, PfTRiC. *Traffic* 16, 461–475.
- Miller, L.H., Baruch, D.I., Marsh, K., and Doumbo, O.K. (2002). The pathogenic basis of malaria. *Nature* 415, 673–679.
- Oberli, A., Slater, L.M., Cutts, E., Brand, F., Mundwiler-Pachlatko, E., Rusch, S., Masik, M.F., Erat, M.C., Beck, H.P., and Vakonakis, I. (2014). A *Plasmodium falciparum* PHIST protein binds the virulence factor PfEMP1 and comigrates to knobs on the host cell surface. *FASEB J.* 28, 4420–4433.
- Oberli, A., Zurbrugg, L., Rusch, S., Brand, F., Butler, M.E., Day, J.L., Cutts, E.E., Lavstsen, T., Vakonakis, I., and Beck, H.P. (2016). *Plasmodium falciparum* *Plasmodium* helical interspersed subtelomeric proteins contribute to cytoadherence and anchor P. falciparum erythrocyte membrane protein 1 to the host cell cytoskeleton. *Cell Microbiol.* 18, 1415–1428.
- Oh, S.S., Voigt, S., Fisher, D., Yi, S.J., LeRoy, P.J., Derick, L.H., Liu, S., and Chishti, A.H. (2000). *Plasmodium falciparum* erythrocyte membrane protein 1 is anchored to the actin-spectrin junction and knob-associated histidine-rich protein in the erythrocyte skeleton. *Mol. Biochem. Parasitol.* 108, 237–247.
- Olaszewski, K.L., Morrisey, J.M., Wilinski, D., Burns, J.M., Vaidya, A.B., Rabinowitz, J.D., and Linas, M. (2009). Host-parasite interactions revealed by *Plasmodium falciparum* metabolomics. *Cell Host Microbe* 5, 191–199.
- Proellocks, N.I., Herrmann, S., Buckingham, D.W., Hanssen, E., Hodges, E.K., Elsworth, B., Morahan, B.J., Coppel, R.L., and Cooke, B.M. (2014). A lysine-rich membrane-associated PHISTb protein involved in alteration of the cytoadhesive properties of *Plasmodium falciparum*-infected red blood cells. *FASEB J.* 28, 3103–3113.
- Przyborski, J.M., Miller, S.K., Pfahler, J.M., Henrich, P.P., Rohrbach, P., Crabb, B.S., and Lanzer, M. (2005). Trafficking of STEVOR to the Maurer's clefts in *Plasmodium falciparum*-infected erythrocytes. *EMBO J.* 24, 2306–2317.
- Quinn, B.J., Welch, E.J., Kim, A.C., Lokuta, M.A., Huttenlocher, A., Khan, A.A., Kuchay, S.M., and Chishti, A.H. (2009). Erythrocyte scaffolding protein p55/MPP1 functions as an essential regulator of neutrophil polarity. *Proc. Natl. Acad. Sci. U S A* 106, 19842–19847.
- Rug, M., Cyrklaff, M., Mikkonen, A., Lemgruber, L., Kuelzer, S., Sanchez, C.P., Thompson, J., Hanssen, E., O'Neill, M., Langer, C., et al. (2014). Export of virulence proteins by malaria-infected erythrocytes involves remodeling of host actin cytoskeleton. *Blood* 124, 3459–3468.
- Salzer, U., and Prohaska, R. (2001). Stomatin, flotillin-1, and flotillin-2 are major integral proteins of erythrocyte lipid rafts. *Blood* 97, 1141–1143.
- Spielmann, T., Hawthorne, P.L., Dixon, M.W., Hannemann, M., Klotz, K., Kemp, D.J., Klonis, N., Tilley, L., Trenholme, K.R., and Gardiner, D.L. (2006). A cluster of ring stage-specific genes linked to a locus implicated in cytoadherence in *Plasmodium falciparum* codes for PEXEL-negative and PEXEL-positive proteins exported into the host cell. *Mol. Biol. Cell* 17, 3613–3624.
- Spillman, N.J., Dalmia, V.K., and Goldberg, D.E. (2016). Exported epoxide hydrolases modulate erythrocyte vasoactive lipids during *Plasmodium falciparum* infection. *MBio* 7, e01538–16.
- Spycher, C., Rug, M., Pachlatko, E., Hanssen, E., Ferguson, D., Cowman, A.F., Tilley, L., and Beck, H.P. (2008). The Maurer's cleft protein MAHRP1 is essential for trafficking of PfEMP1 to the surface of *Plasmodium falciparum*-infected erythrocytes. *Mol. Microbiol.* 68, 1300–1314.
- van der Meer-Janssen, Y.P., van Galen, J., Batenburg, J.J., and Helms, J.B. (2010). Lipids in host-pathogen interactions: pathogens exploit the complexity of the host cell lipidome. *Prog. Lipid Res.* 49, 1–26.
- Waller, K.L., Cooke, B.M., Nunomura, W., Mohandas, N., and Coppel, R.L. (1999). Mapping the binding domains involved in the interaction between the *Plasmodium falciparum* knob-associated histidine-rich protein (KAHRP) and the cytoadherence ligand P. falciparum erythrocyte membrane protein 1 (PfEMP1). *J. Biol. Chem.* 274, 23808–23813.
- Waller, K.L., Muhle, R.A., Ursos, L.M., Horrocks, P., Verdier-Pinard, D., Sidhu, A.B., Fujioka, H., Roepe, P.D., and Fidock, D.A. (2003). Chloroquine resistance modulated in vitro by expression levels of the *Plasmodium falciparum* chloroquine resistance transporter. *J. Biol. Chem.* 278, 33593–33601.
- Wang, J., Zhang, C.J., Chia, W.N., Loh, C.C., Li, Z., Lee, Y.M., He, Y., Yuan, L.X., Lim, T.K., Liu, M., et al. (2015). Haem-activated promiscuous targeting of artemisinin in *Plasmodium falciparum*. *Nat. Commun.* 6, 10111.
- Watanabe, T., Kawakami, E., Shoemaker, J.E., Lopes, T.J., Matsuoka, Y., Tomita, Y., Kozuka-Hata, H., Gorai, T., Kuwahara, T., Takeda, E., et al. (2014). Influenza virus-host interactome screen as a platform for antiviral drug development. *Cell Host Microbe* 16, 795–805.
- WHO (2018). WHO | World malaria report, Available at: <http://www.who.int/malaria/publications/world-malaria-report-2018/en/>, Accessed: 30th June 2019.
- Wickham, M.E., Rug, M., Ralph, S.A., Klonis, N., McFadden, G.I., Tilley, L., and Cowman, A.F. (2001). Trafficking and assembly of the cytoadherence complex in *Plasmodium falciparum*-infected human erythrocytes. *EMBO J.* 20, 5636–5649.

ISCI, Volume 19

## Supplemental Information

### A High-Resolution

### Map of SBP1 Interactomes

### in *Plasmodium falciparum*-infected Erythrocytes

Ryo Takano, Hiroko Kozuka-Hata, Daisuke Kondoh, Hiroki Bochimoto, Masaaki Oyama, and Kentaro Kato

## Supplementary Information

### Supplementary figures

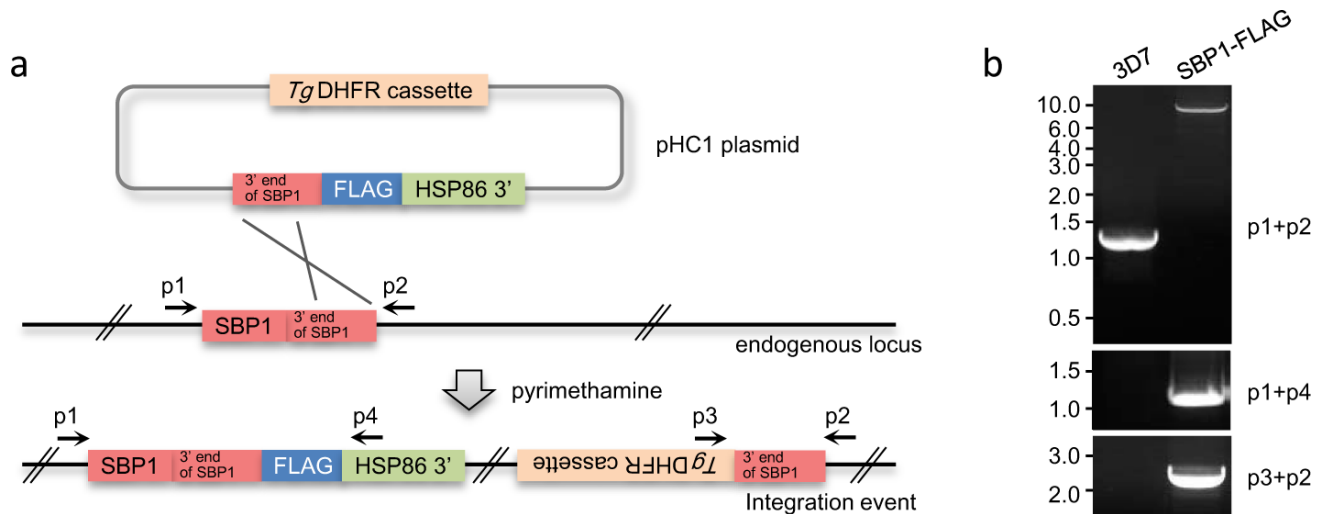


**Figure S1. Generation of endogenous SBP1-FLAG parasite transfectants., Related to Figures 1 and 2.**

(a) Schematic of targeting construct designed to integrate into the endogenous *SBP1* locus by single crossover recombination. Arrows indicate positions of oligonucleotide primers used to confirm integration. *TgDHFR*, *Toxoplasma gondii* dihydrofolate reductase. (b) Diagnostic PCR analysis of wild-type 3D7 and SBP1-FLAG transfectant parasite lines. Oligonucleotide pair p1/p2 amplifies the endogenous locus, whereas oligonucleotide pairs of p1/p4 and p3/p2 amplify the transgenic locus. DNA size is shown in kbp.

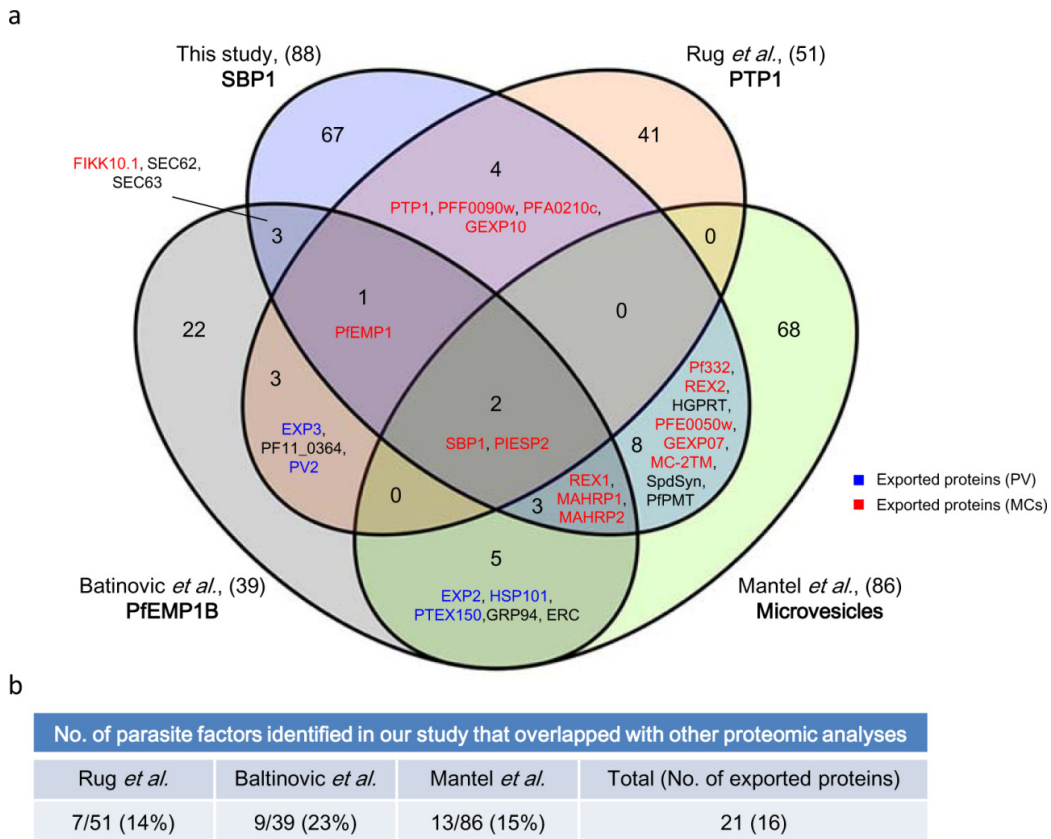


**Figure S2. Comparison of the 88 parasite proteins identified in our study with the proteins identified in three independent proteomic analyses for exported proteins (PfEMP1 and PTP1) associated with the trafficking complex and microvesicles. Related to Figures 1 and 2.**

(a) Venn diagram of the parasite factors identified as interacting with SBP1 in our study and in previous proteomics studies (Batinovic *et al.*, 2017; Mantel *et al.*, 2013; Rug *et al.*, 2014). Shown are the total numbers of parasite factors that overlapped in these studies. The proteins exported to the parasitophorous vacuole (PV) and Maurer's clefts (MCs) are colored by blue and red, respectively. (b) Numbers of proteins and exported proteins identified in this study that overlapped with other studies. The dataset reported by Mantel *et al.* contains the highest number (13 proteins) of proteins that were also identified by us, suggesting that microvesicles are highly likely to originate from Maurer's clefts. By contrast, the study by Rug *et al.* identified a small number of proteins (6 proteins; PfEMP1, SBP1, PIESP2, EXP3, PV2, and PF11\_0364) that were also identified by Batinovic *et al.* despite both studies being conducted on the same trafficking complex that included PfEMP1 and SBP1, possibly due to differences in the co-immunoprecipitation systems used. The abundance and variety of exported proteins identified by us demonstrate that our SBP1 interactomes could serve as intermediaries to connect previous proteomic studies (Batinovic *et al.*, 2017; Rug *et al.*, 2014).

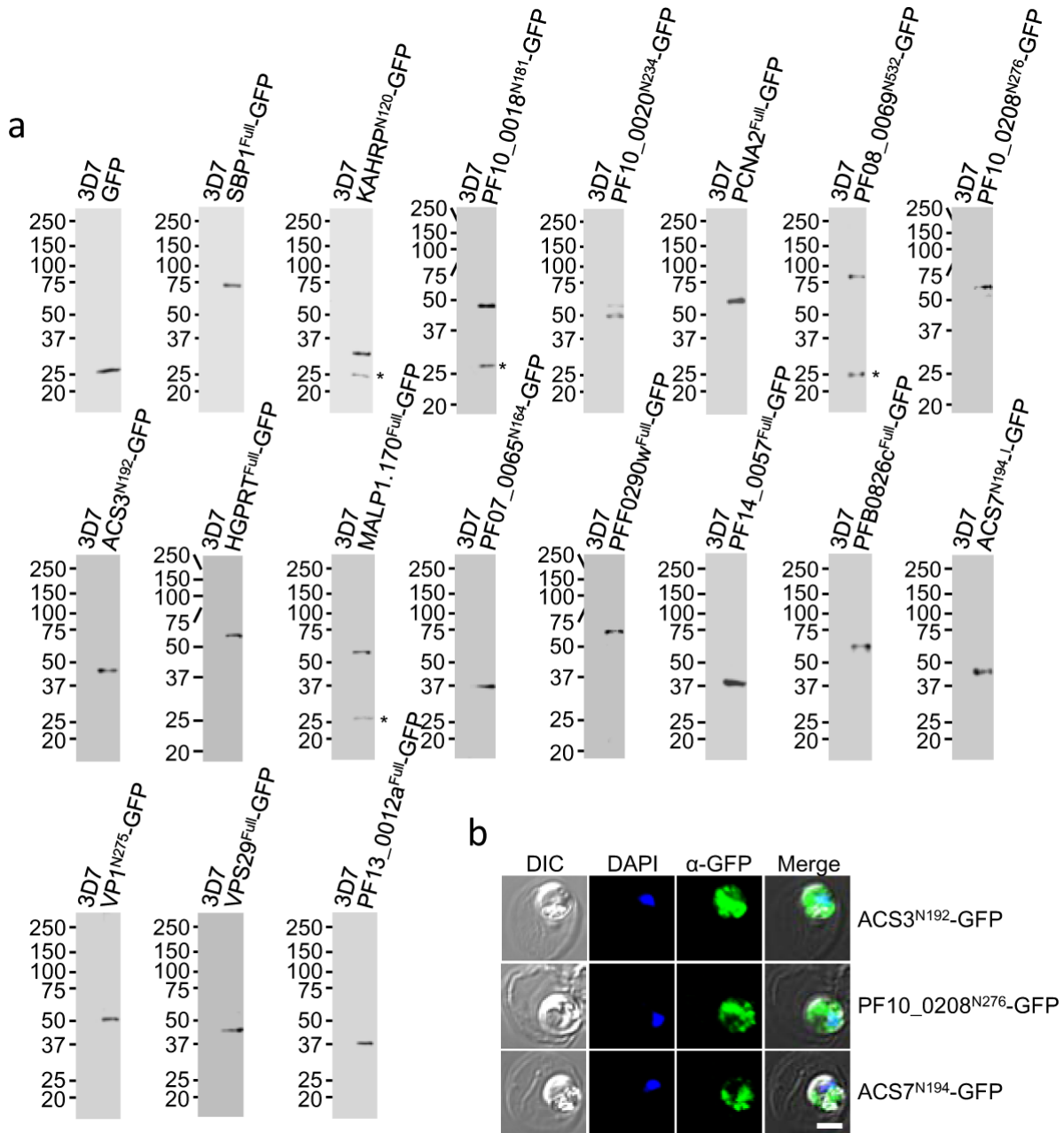
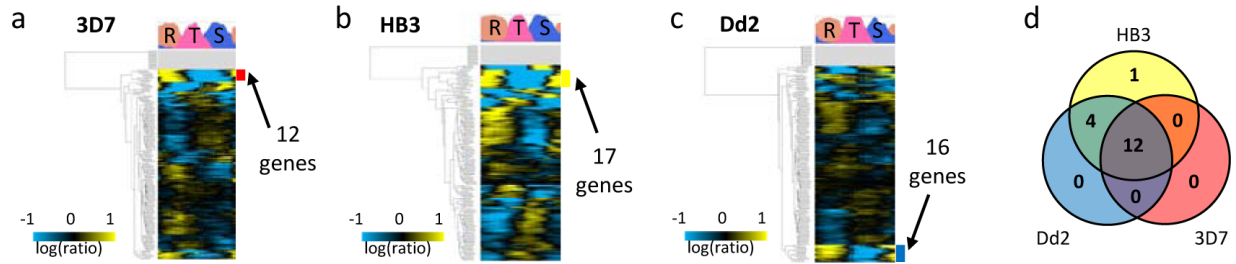


**Figure S3. Expression of transgenic parasite cell lines used in the GFP-based protein export assay., Related to Figure 4.**

(a) Western blots of extracts from the transgenic cell lines. Origins of the individual extracts are indicated above each blot. Protein size is shown in kDa. Asterisks indicate degradation products of the GFP-fused protein, likely representing GFP alone. (b) Immunofluorescence assay of three transgenic cell lines showing weak GFP fluorescence in live cell imaging analysis. The GFP-fused proteins were stained with anti-GFP antibodies (green), whereas DAPI (blue) was used to stain the nuclei. Scale bar: 3  $\mu$ m.



**e**

	Accession	Previous IDs	Description	Mascot Protein Score		Gene disrupted	References
				SBP1-FLAG	3D7		
25 high ranked genes	PF3D7_0501300	PFE0065w	Skeleton-binding protein 1 (SBP1)	10064.58	75.39	Yes	Cooke BM et al., 2006, JCB
	PF3D7_1240900	PFL1970w	Erythrocyte membrane protein 1, PFEMP1 (VAR)	1382.09	-	-	-
	PF3D7_1149000	PF11_0507	Antigen 332, DBL-like protein (PF332)	3525.83	40.49	Yes	Maier AG et al., 2008, Cell
	PF3D7_0501200	PFE0060w	Parasite-infected erythrocyte surface protein (PIESP2)	987.37	-	Yes	Maier AG et al., 2008, Cell
	PF3D7_1001400	PF10_0018	Alpha/beta hydrolase, putative	545.14	-	Yes	In this study
	PF3D7_1001600	PF10_0020	Alpha/beta hydrolase, putative	436.20	-	-	-
	PF3D7_1253400	PFL2570w	Acyl-CoA synthetase (ACS3)	425.29	-	No	In this study
	PF3D7_1226600	PFL1285c	Proliferating cell nuclear antigen 2 (PCNA2)	401.87	-	Yes	Leiden University
	PF3D7_0832200.1	MAL7P1.225	Plasmodium exported protein (PHISTA-like), unknown function	365.55	-	-	-
	PF3D7_1357700	PF13_0309	U3 snRNA-associated small subunit rRNA processing protein, putative	252.04	-	No	In this study
	PF3D7_1141300	PF11_0424	Conserved Plasmodium protein, unknown function	250.00	-	-	-
	PF3D7_0815200	PF08_0069	Importin beta, putative	246.41	-	No	In this study
	PF3D7_1012400	PF10_0121	Hypoxanthine-guanine phosphoribosyltransferase (HGPRT)	240.95	-	-	-
	PF3D7_1311900	PF13_0065	Vacuolar ATP synthase subunit a (vapA)	222.69	-	No	In this study
	PF3D7_0700800	MAL8P1.213	Pfmc-2TM Maurer's cleft two transmembrane protein (MC-2TM)	198.62	-	-	-
	PF3D7_0501000	PFE0050w	Plasmodium exported protein, unknown function	189.85	-	Yes	Maier AG et al., 2008, Cell
	PF3D7_1021400	PF10_0208	Endomembrane protein 70, putative	187.73	-	-	-
	PF3D7_0715900	PF07_0065	Zinc transporter, putative	183.60	-	Yes	Leiden University
	PF3D7_1039000	PF10_0380	Serine/threonine protein kinase, FIKK family (FIKK10.2)	183.16	-	Yes	In this study
	PF3D7_0824400	MAL8P1.32	Nucleoside transporter 2 (NT2)	181.12	-	Yes	Leiden University
	PF3D7_0936000	PF11740c	Ring-exported protein 2 (REX2)	244.20	-	-	-
	PF3D7_1370300	MAL13P1.413	Membrane associated histidine-rich protein (MAHRP1)	233.71	-	Yes	Spycher C et al., 2008, MM
	PF3D7_0935900	PF11735c	Ring-exported protein 1 (REX1)	216.10	-	Yes	Dixon MWA et al., 2011, MM
	PF3D7_0202200	PFB0106c	EMP1-trafficking protein (PTP1)	214.28	-	Yes	Rug M et al., 2014, Blood
	PF3D7_0730800.1	MAL7P1.170	Plasmodium exported protein, unknown function	197.62	-	Yes	Maier AG et al., 2008, Cell
PF3D7_0830500	PF08_0003	Tryptophan/threonine-rich antigen (TryThrA)	162.05	-	Yes	In this study	
PF3D7_1200700	PFL0035c	Acyl-CoA synthetase (ACS7)	136.42	-	No	In this study	
PF3D7_1456800	PF14_0541	V-type H(+)-translocating pyrophosphatase, putative (VP1)	126.20	-	No*	In this study	
PF3D7_0702300	PF07_0006	Sporozoite threonine and asparagine-rich protein (STARP)	119.61	-	Yes	In this study	
PF3D7_1301700	MAL13P1.61	Plasmodium exported protein (hyp8), unknown function (GEXP07)	89.12	-	No	Maier AG et al., 2008, Cell	
PF3D7_1353100	PF13_0275	Plasmodium exported protein, unknown function	81.61	-	Yes	Maier AG et al., 2008, Cell	
PF3D7_1252600	PFL2530w	Lysophospholipase, putative	60.06	-	Yes	In this study	
PF3D7_1404800	PF14_0045	Conserved Plasmodium protein, unknown function	59.84	-	No	In this study	
PF3D7_0830600	MAL8P1.4	Plasmodium exported protein (PHISTc), unknown function	59.70	-	Yes	In this study	
PF3D7_1002100	PF10_0025	PF70 protein (PF70) / EMP1-trafficking protein (PTP5)	58.77	-	Yes	Maier AG et al., 2008, Cell	
PF3D7_0219900	PFB0910w	Plasmodium exported protein, unknown function	32.98	-	-	-	
PF3D7_1319100	PF13_0106	Conserved protein, unknown function	32.25	-	-	-	
17 ring-stage specific expressed genes							

**Figure S4. Selection of genes for knockout screening., Related to Figure 5.** To identify genes involved in the cytoadherence of iRBCs to vascular endothelial receptors, we first selected genes that are specifically expressed in the ring stage of parasites. Expression data for 205 genes shown in Table S2 were retrieved from DeRisi's microarray data available in PlasmoDB (<http://plasmodb.org/plasmo/>), and were analyzed for each parasite strain based on expression similarity. The number of ring-specific genes was 12, 17, and 16, for 3D7 (a), HB3 (b), and Dd2 (c), respectively. (d) Venn diagram showing the overlap of ring-specific genes across the three parasite strains. (e) Gene candidates selected for knockout screening. A total of 37 genes, 17 ring-specific genes plus the 25 top-ranked genes from Table S3, were selected for knockout screening. Shown in the first through fourth columns are the accession number, previous genes IDs, gene description, and Mascot Protein Scores of each protein in the SBP1-FLAG and 3D7 proteome. The fifth and sixth columns indicate whether the gene can be genetically disrupted (Yes) or not (No), and the references in which knockout attempts had been previously performed.

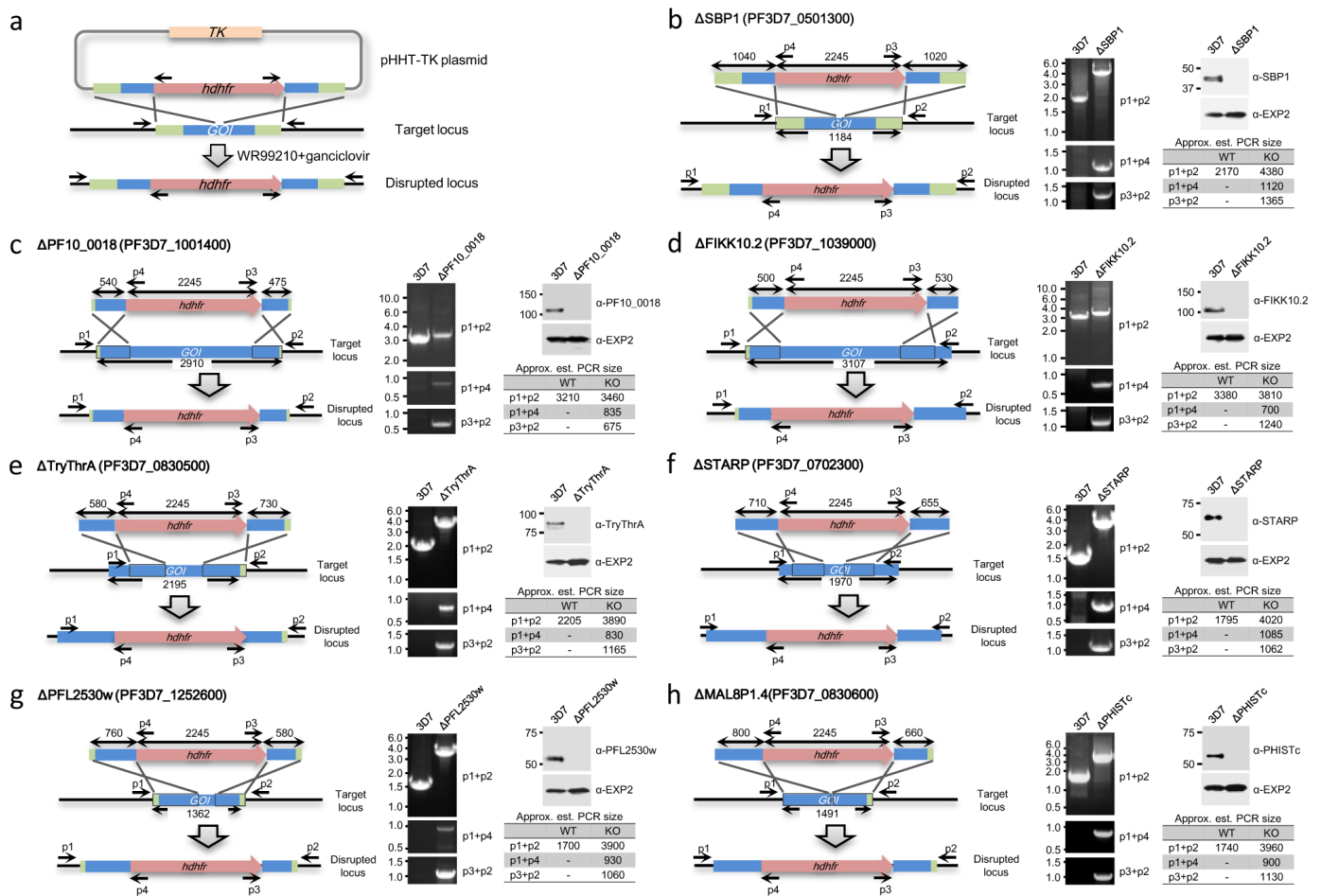


**Figure S5. Genetic disruption of seven genes that were disrupted., Related to Figures 5, S4 and S6.**

(a) Schematic of targeting construct designed to delete genes of interest (GOI) by double homologues recombination. Arrows indicate positions of oligonucleotide primers used to confirm replacement targeting events. TK, Thymidine kinase; *hdhfr*, human dihydrofolate reductase. (b–h) Strategies of genetic disruption, diagnostic PCR, and western blot analyses are shown for each gene. The replacement of the native gene locus with a targeting vector, and the absence of protein expression in transgenic parasite lines in which the genes *SBP1* (b), *PF10\_0018* (c), *FIKK10.2* (d), *TryThrA* (e), *STARP* (f), *PFL2530w* (g), and *MAL8P1.4* (g) had been disrupted were confirmed by PCR and western blot analyses, respectively. Primers used in the study are summarized in Table S5. DNA and protein sizes are shown in kbp and kDa, respectively. The wild-type 3D7 is shown in each panel and equal loading is demonstrated with anti-EXP2 antibodies.

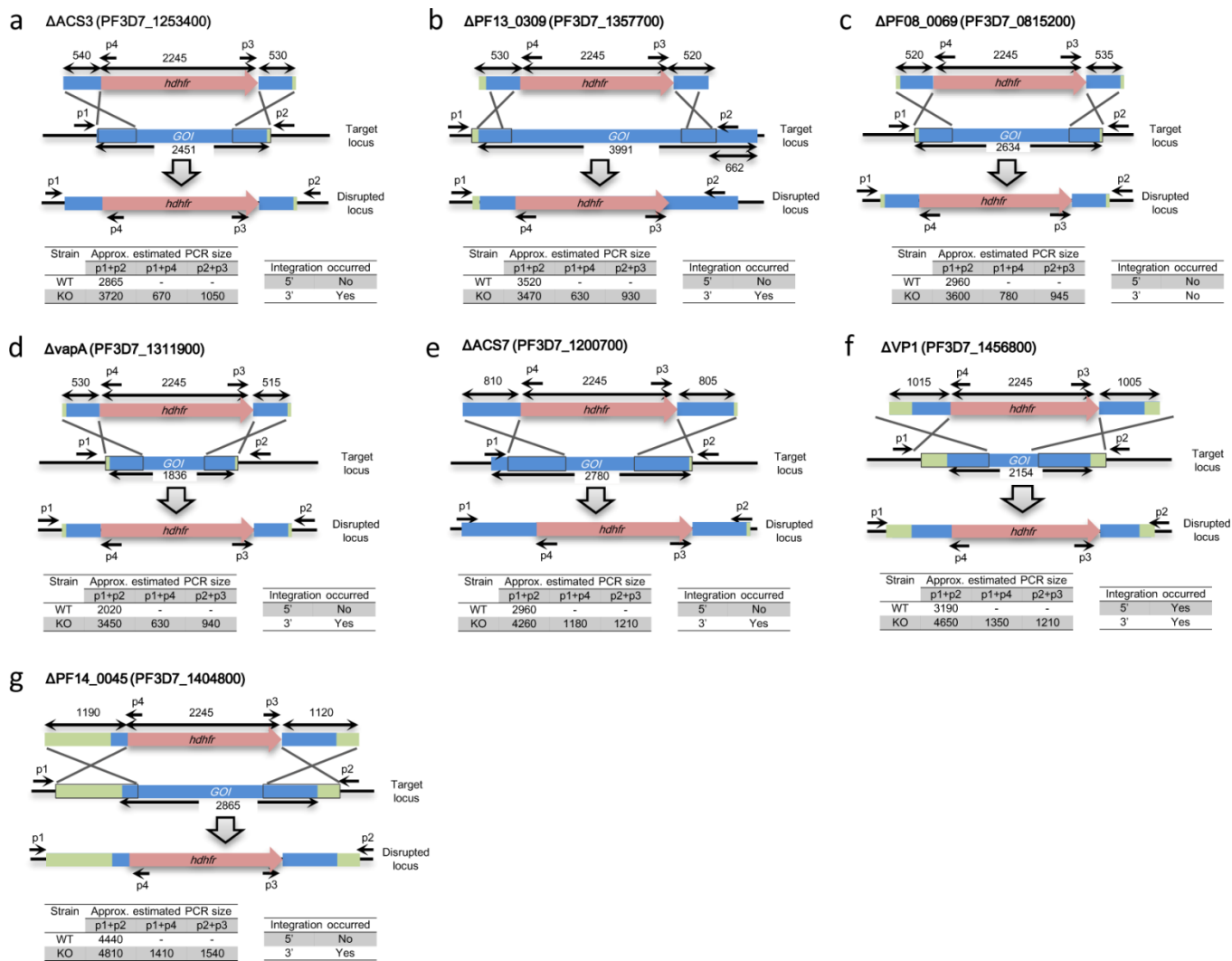


**Figure S6. Targeting constructs designed to disrupt the seven genes that are likely essential for parasites in asexual blood development., Related to Figures 5, S4 and S5.**

Plasmids were transfected into parasites, and the transfectants were selected by WR99210 and ganciclovir to favor the survival of transfected parasites with double homologous integration into the target gene and loss of episomal plasmids. Diagnostic PCR analyses were then conducted for the genomic DNAs extracted from genetically heterogeneous population of parasites before limiting dilution; the PCR results refer to whether the homologous recombination for the 5' and 3' ends of the endogenous gene had occurred (Yes) or no (No). The knockout attempts were independently conducted three times. For the *VP1* gene (PF3D7\_1456800), we were able to confirm that homologous recombination for both the 5' and 3' ends of endogenous *VP1* gene had occurred in the transfectants of the genetically heterogeneous population before limiting dilution; however, we failed to obtain parasite clones by limiting dilution presumably because of the delayed growth of the parasites.

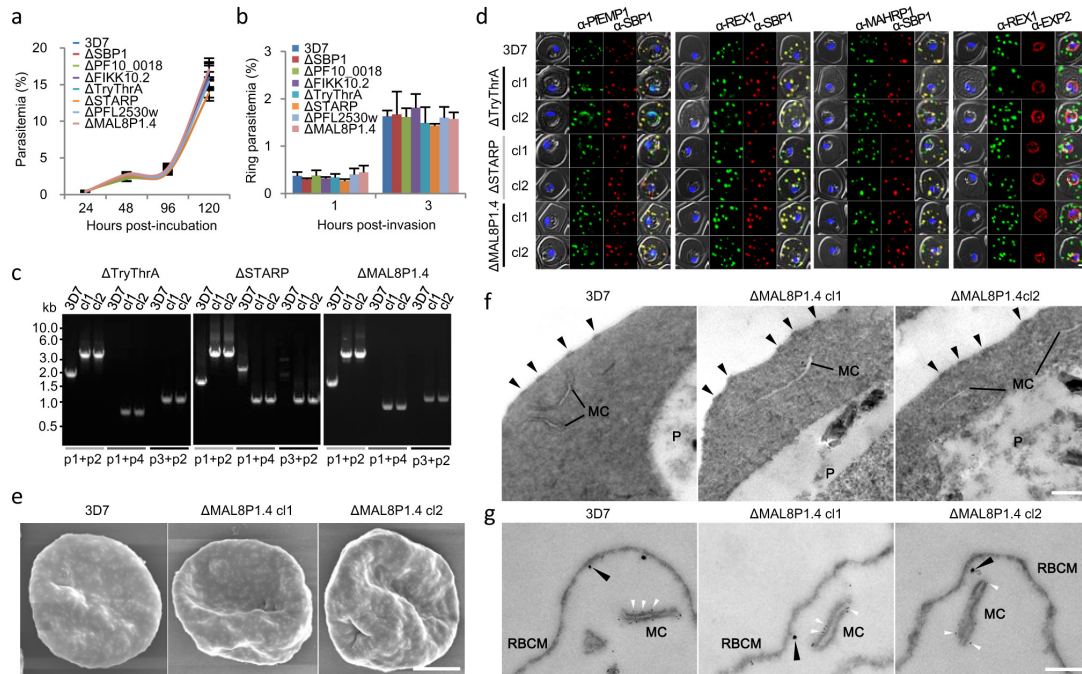


**Figure S7. Phenotypic examination of erythrocytes infected with knockout mutants., Related to Figure 5.**

(a and b) The growth and invasion of seven mutant parasites obtained in the asexual stage of development. (c) Diagnostic PCR on *P. falciparum* 3D7 and 3 knockout mutants using specific primers to confirm the integration of the targeting constructs. Schematics of the targeting constructs designed to disrupt the endogenous *TryThrA*, *STARP*, and *MAL8P1.4* loci are shown in Fig. S5e, f, and h, respectively. Two clones for each knockout cell line were isolated by limiting dilution and analyzed. (d) Immunofluorescence assays of erythrocytes infected with *P. falciparum* 3D7 and 3 knockout mutants. iRBCs were probed with  $\alpha$ -PfEMP1,  $\alpha$ -MAHRP1, and  $\alpha$ -REX1 to test their localization in Maurer's clefts.  $\alpha$ -SBP1 and  $\alpha$ -EXP2 were used as markers for Maurer's clefts and parasitophorous vacuole (PV), respectively. Scale bar: 2 nm. (e) SEM of erythrocytes infected with two clones of  $\Delta$ *MAL8P1.4* parasites. The first panel shows parental 3D7-infected erythrocytes with normal knobs compared to the two mutant clones. Scale bars: 2  $\mu$ m. (f) TEM of erythrocytes infected with  $\Delta$ *MAL8P1.4* parasites. Parental 3D7-infected erythrocytes with normal knobs and normal morphology of Maurer's clefts were compared to  $\Delta$ *MAL8P1.4* mutants in which no apparent changes were observed in the morphology of the erythrocyte surface or the Maurer's clefts. Arrowhead indicates knobs; MC, Maurer's cleft; P, parasites. Scale bar: 200 nm. (g) Double-stained immunoelectron microscopy of tetanolysin-permeabilized iRBCs to examine the localization of SBP1 and PfEMP1, which were labeled with 5-nm and 15-nm gold particles, respectively. PfEMP1 signal (black arrowhead) was detected at the erythrocyte surface, whereas SBP1 (white arrowhead) was detected in Maurer's clefts. MC indicates Maurer's clefts; RBCM, red blood cell membrane. Scale bar: 200 nm.

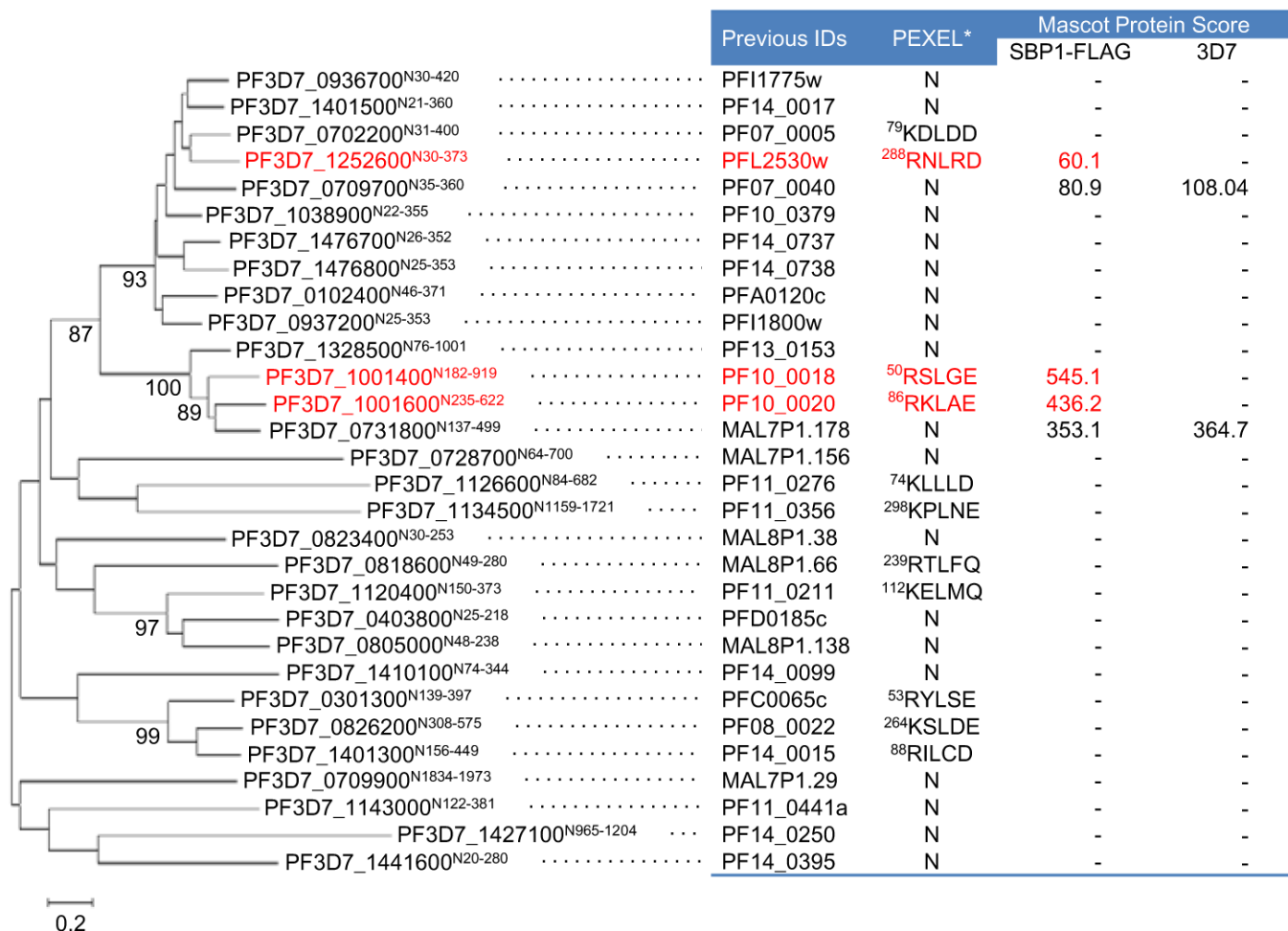


**Figure S8. Genetic diversity and phylogenetic relationships of parasite proteins with the  $\alpha/\beta$  hydrolase domain. Related to Figures 4 and 5.**

The sequences of 30 genes that encode proteins predicted to possess the  $\alpha/\beta$  hydrolase domain were retrieved from PlasmoDB (<http://plasmodb.org/plasmo/>). The protein coding regions of the  $\alpha/\beta$  hydrolase domain are shown in subscript for each protein and were phylogenetically analyzed by using the neighbor-joining method. The bootstrap values are shown at the node of branches. \*N-terminally closest PEXEL sequences [(R/K)xLx(D/E/Q)] found in the regions within 300 amino acids of the N-terminus are shown. N: not presented. The proteins identified as SBP1-binding factors in this study are shown in red.

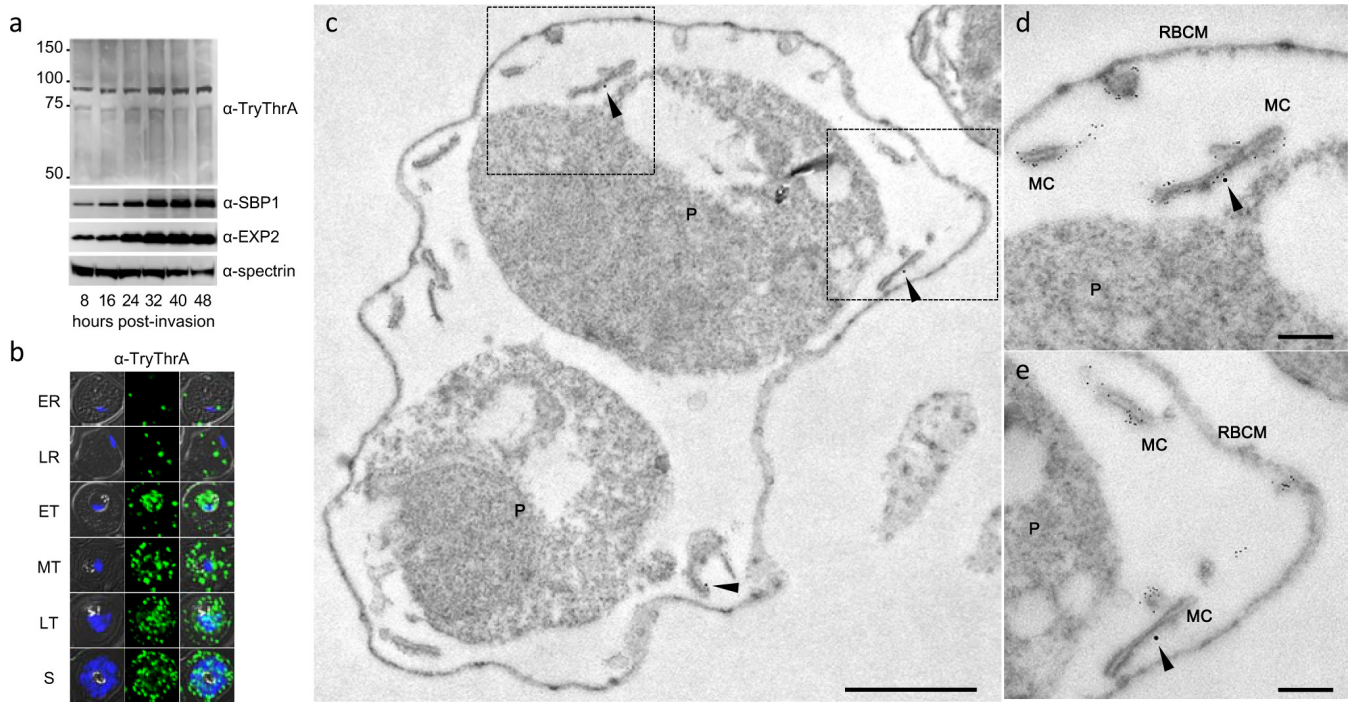


**Figure S9. Expression and localization of TryThrA in *P. falciparum*-infected erythrocytes., Related to Figure 5.**

(a) TryThrA expression during the intracellular cycle (8–48 hours) in infected erythrocytes. Tightly synchronized *P. falciparum* 3D7-infected RBCs were collected every 8 hours, lysed with saponin, and equivalent amounts of pellets were analyzed by western blotting. (b) Localization of TryThrA during the intracellular cycle by immunofluorescence assessment. The fixed cells were reacted with  $\alpha$ -TryThrA antibody. Parasite nucleus was stained with DAPI. ER, early ring; LR, late ring; ET, early trophozoite; MT, middle trophozoite; LT, late trophozoite; S, schizont. (c–e) Double-stained immunoelectron microscopy of tetanolysin-permeabilized iRBCs to confirm the localization of TryThrA in Maurer's clefts. SBP1 and TryThrA were labeled with 5-nm and 15-nm gold particles, respectively. Arrowhead indicates TryThrA; MC, Maurer's clefts; P, parasites; RBCM, red blood cell membrane. Scale bars: 1  $\mu$ m (c) and 200 nm (d and e), respectively.

## Transparent Methods

### *Ethics statement.*

Our research protocol for the use of human-derived samples was approved by the Research Ethics Review Committee, Obihiro University of Agriculture and Veterinary Medicine (approval number 2013-04).

### *Parasites and cell culture.*

The *P. falciparum* 3D7 clone was obtained from the Malaria Research and Reference Reagent Resource Center (MR4; American Type Culture Collection, Manassas, VA). The parasites were continuously cultured in RPMI/HEPES medium (Sigma-Aldrich) supplemented with 100  $\mu$ M hypoxanthine (Wako), 10  $\mu$ g/ml gentamycin (Sigma-Aldrich), 1.5 mg/ml NaHCO<sub>3</sub> (Wako), and 5 mg/ml Albumax II (Invitrogen), as described previously (Trager and Jensen, 2005). Parasites were synchronized either by D-sorbitol (Wako) treatment (Lambros and Vanderberg, 1979), by Percoll (GE Healthcare) gradient (Kramer et al., 1982), by MACS separation (Ribaut et al., 2008) (LD column, Miltenyi Biotec), and/or by gelatin floatation (Jensen, 1978). Human RBCs (blood type A+, O+, or AB+) were obtained from healthy volunteers under appropriate informed consent, and used in the study.

### *DNA and RNA extractions.*

Parasite lysates were prepared by saponin lysis of parasite-infected erythrocytes, as essentially described previously (Boddey et al., 2016). Genomic DNA and total RNAs were extracted from parasite lysates by using the Nucleospin Tissue (Marcherey-Nagel), and SV Total RNA Isolation System (Promega), respectively. Extracted total RNA was reversely transcribed to cDNA with oligo(dT) primers and SuperScript<sup>TM</sup> III reverse transcriptase (Invitrogen) according to the manufacturer's instructions.

### *Transgenic parasites.*

To generate parasites episomally expressing C-terminally FLAG- or GFP-tagged proteins, the protein coding regions of interest were amplified from parasite cDNA using the specific primers listed in Table S5, and cloned into the expression vectors C-Flag-pHC1 or pARL1-GFP, respectively. C-Flag-pHC1 vector, which encodes a FLAG epitope and an upstream site for the generation of FLAG-tagged proteins, was generated based on the pHC1 vector (Crabb et al., 1997), which contains the *DHFR-TS* gene that encodes resistance to pyrimethamine. The pARL1-GFP vector, which expresses GFP-tagged proteins under the control of the *crt* promoter and contains the *hDHFR* gene that confers resistance to WR99210, was generated based on

the pARL1-*KAHRP-GFP* vector (Knuepfer et al., 2005; Marti et al., 2004), which was a kind gift from Dr. Alan F. Cowman (Walter and Eliza Hall Institute, Australia). Briefly, the vector was cut with *Xho*I to remove the *KAHRP-GFP* fragment, and the protein coding regions to be tested were PCR-amplified and either inserted into the *Xho*I site of the vector simultaneously with PCR-amplified GFP fragments using an In-Fusion Cloning kit (Clontech), or were subcloned into the *Not*I site of the C-GFP-pHC1 vector, which encodes GFP and an upstream site for the generation of GFP-tagged proteins. In the latter, the coding regions of the GFP-fused proteins were further PCR-amplified and cloned into the corresponding sites of pARL1. To generate parasites expressing FLAG-tagged SBP1 under the control of the endogenous promoter, the 3'-terminal genomic region of *SBP1* (~1.0 kb) was PCR-amplified from parasite genomic DNAs, and cloned into the C-Flag-pHC1 vector as described above. For the generation of knock-out mutants, the allelic exchange fragments composed of approximately 0.6–1.0 kb were PCR-amplified from parasite genomic DNAs, and cloned into the *Sac*II/*Spe*I and *Eco*RI/*Nco*I sites of the pHHT-TK vector, which contains the *hDHFR* cassette and a negative selection cassette to select parasites in which double recombination events had occurred (Duraisingh et al., 2002). PCR was carried out by using KOD-plus-DNA polymerase (TOYOBO, Japan), and the plasmid DNA was extracted using Maxiprep kits (Invitrogen). Prior to use, all of the plasmids were sequenced to ensure the absence of any unwanted mutations.

Plasmid transfection was conducted by electroporation as previously described (Waller et al., 2003). Briefly, red blood cells were pre-loaded with 50–200 µg of plasmid DNAs, and mixed with purified late stage parasites at a final parasitemia of 0.1%. Transfectants were selected by the addition of 50 nM pyrimethamine (Sigma-Aldrich) or 5 nM WR99210 (Jacobus Pharmaceuticals) to the culture medium, starting 72 h post-transfection. Once the transgenic parasites were established, the drug concentration was increased to 2 µM pyrimethamine or 20 nM WR99210. To obtain knock-out parasites, the genomes of which were replaced by vector sequences, parasites after positive selection on WR99210 were placed under negative selection using 4 µM ganciclovir (Wako) in addition to WR99210. If no parasites were recovered, the negative selection was repeated at least twice. Mutant parasites were cloned by limiting dilution and at least two clones for each mutant were used for subsequent analyses.

### **Generation of recombinant proteins and antiserum.**

The antibodies against parasite proteins were generated by immunization of mice with recombinant proteins expressed by the Wheat Germ Cell-Free System (WGCFS, Cell-Free Inc., Japan) as described (Tsuboi et al., 2008). Briefly, the protein coding regions of the following 14 genes were PCR-amplified with the indicated primers listed in Table S5: *PfEMP1* (PF3D7\_1240900, 5458–6861 of 6864 bp), *PIESP2* (PF3D7\_0501200, 136–1224 of 1227 bp),

*PF10\_0018* (PF3D7\_1001400, 160–2548 of 2766 bp), *REX1* (PF3D7\_0935900, 163–2139 of 2142 bp), *REX2* (PF3D7\_0936000, 16–282 of 285 bp), *REX3* (PF3D7\_0936300, 160–471 of 981 bp), *MAHRP1* (PF3D7\_1370300, 4–747 of 750 bp), *MAHRP2* (PF3D7\_0324600, 4–411 of 414), *STEVOR* (PF3D7\_0324600, 151–903 of 906 bp), *TryThrA* (PF3D7\_0830500, 1288–2022 of 2028 bp), *FIKK10.2* (PF3D7\_1039000, 271–2115 of 2742 bp), *STARP* (PF3D7\_0702300, 1081–1638 of 1785 bp), *PFL2530w* (PF3D7\_1252600, 991–1347 of 1362 bp), and *MAL8P1.4* (PF3D7\_0830600, 418–975 of 1371 bp). The PCR products were subsequently inserted into the *Bam*HI/*Not*I sites of the pEU-GST-MCS vector, which encodes GST to express N-terminal GST-fusion proteins. The constructed plasmids were extracted and purified with Midiprep Kits (Invitrogen) followed by the phenol-chloroform method to remove residual RNase contamination, and used to synthesize recombinant proteins using the WEPRO1240G Expression Kit (Cell-Free Inc.). *In vitro* transcription, translation, and purification of recombinant proteins were conducted according to the manufacturer's instructions.

A mouse (5- to 8-week-old female BALB/c strain, CLEA Japan, Inc.) was injected subcutaneously with 2–20 µg of each purified recombinant protein with Titermax Gold Adjuvant (Funakoshi), and the immunization was boosted at 7–10 day intervals three times. If necessary, a booster immunization was given up to 5 times to obtain polyclonal mouse serum. The antisera were tested for specificity prior to use by immunoblot analyses on cell lysates prepared from MACS-purified or saponin-treated erythrocytes, and by immunofluorescence analyses of blood smears of parasite-infected erythrocytes.

### **Antibodies.**

The mouse and rabbit anti-SBP1, and the rabbit anti-EXP2 antibodies were kind gifts from Dr. Takafumi Tsuboi (Ehime University, Japan). The mouse anti-FLAG epitope tag (F1804, Sigma-Aldrich), anti-FLAG M2-Affinity Gel (A2220, Sigma-Aldrich), mouse anti-GFP (mFX73, Wako), mouse anti-spectrin ( $\alpha$  and  $\beta$ ) (S3396, Sigma-Aldrich), rabbit anti-STOM (HPA010961, Atlas Antibodies), rabbit anti-KPNB1 (LS-B11745, LifeSpan Biosciences Inc.), and mouse anti-MPP1 (ab55464, Abcam; SAB1404080, Sigma-Aldrich) were purchased from the commercial sources indicated. The polyclonal antisera raised from mice immunized with the recombinant parasite antigens described above were available in our laboratory. The following antibodies were used as secondary antibodies: goat anti-mouse IgG Alexa 488 (A11001, Life Technologies), goat anti-rabbit IgG Alexa 488 (A11008, Life Technologies), donkey anti-mouse IgG Alexa 594 (A21203, Life Technologies), goat anti-rabbit IgG Alexa 594 (A11037, Life Technologies), HRP-conjugated anti-mouse IgG antibody (NA9310V, GE Healthcare), HRP-conjugated anti-rabbit IgG antibody (NA9340V, GE Healthcare), gold-conjugated (15 nm) goat anti-mouse IgG (AC-15-02-05, Cytodiagnosics), gold-conjugated (5 nm) goat anti-rabbit

IgG (AC-5-01-05, Cytodiagnosics) antibodies, and gold-conjugated (5 nm) Protein G (AC-5-18-05). The following antibodies were used only for western blotting: HRP-conjugated mouse anti-FLAG (A8592, Sigma-Aldrich), HRP-conjugated rabbit anti-GFP (598-7, MBL), HRP-conjugated rabbit anti-GST tag (PM013-7, MBL), and HRP-conjugated mouse anti-His tag (D291-7, MBL) antibodies.

### ***Immunoprecipitation and mass spectrometry analysis.***

Immunoprecipitation followed by shotgun proteomics were carried out as previously described (Gorai et al., 2012; Watanabe et al., 2014) with some modifications. Briefly, 100 µl of MACS-purified erythrocytes (> 90% infected cells) were incubated with lysis buffer [50 mM Tris-HCl (pH 8.0) (Invitrogen), 150 mM NaCl (Ambion), 2.0% Nonidet P-40 (NP-40, Sigma-Aldrich), and protease inhibitors (Complete Mini, Roche)] for 1 h at 4 °C. After clarification by centrifugation to remove cellular debris, the supernatants were incubated with an anti-FLAG M2-Affinity Gel (Sigma-Aldrich) for 17 h at 4 °C. The affinity gels were washed thoroughly with lysis buffer without protease inhibitors, and then washed twice with immunoprecipitation (IP) buffer (50 mM Tris-HCl and 150 mM NaCl). Proteins bound to affinity gels were eluted with elution buffer [50 mM Tris-HCl, 150 mM NaCl, and 0.5 mg/ml FLAG peptide (Sigma-Aldrich)] for over 4 h at 4 °C. After the gel was removed by centrifugation, the supernatants were filtered by using an Ultrafree-MC filter (Millipore). Filtered samples were subjected to SDS/PAGE followed by silver staining, western blotting, or mass spectrometric analysis.

For mass spectrometric comprehensive detection, eluted proteins were trypsinized and subjected to shotgun proteomic analyses to identify co-immunoprecipitated proteins. For this analysis, we used a linear ion trap-orbitrap mass spectrometer (LTQ-Orbitrap Velos, Thermo Fisher Scientific) coupled with a nanoflow LC system (Dina-2A, KYA Technologies). Protein identification was performed by searching MS and MS/MS data against the RefSeq (National Center for Biotechnology Information) human protein database together with PlasmoDB (Plasmodium Genomic Resource), the *Plasmodium falciparum* protein database, using Mascot ver. 2.4.1 (Matrix Science) with the following parameters: variable modifications, oxidation of methionine, protein N-terminal acetylation, pyro-glutamination for N-terminal glutamine; maximum missed cleavages, 2; peptide mass tolerance, 3 ppm; MS/MS tolerance, 0.8 Da. In the process of peptide identification, we conducted decoy database searches using Mascot and applied a filter to satisfy a false positive rate lower than 1%.

### ***Bioinformatics.***

To ensure the comparability of the two proteomic datasets, we first statistically compared the

power of detection and proteome coverage for the proteomic data obtained from 3D7-infected erythrocytes with those obtained from SBP1-FLAG-infected erythrocytes. Mascot protein scores and their distributions were analyzed by using Mann-Whitney's U and Kolmogorov-Smirnov tests, respectively. A protein was considered an SBP1-interacting candidate if it satisfied either of two different criteria, resulting in two datasets, that is, one set containing proteins that were identified only in the SBP1-FLAG proteome and not in the 3D7 proteome (number of proteins = 256; median Mascot protein score = 61.1, Table S2), and the second containing proteins with a fold change greater than 5.0 (corresponding to  $\sim 1.5\sigma$  for Gaussian variables) in Mascot protein scores of the SBP1-FLAG proteome relative to those of the 3D7 proteome (number of proteins = 106; median Mascot score = 157.1, Table S3). Functional enrichment analyses of the SBP1-interacting factors were carried out using the Gene Ontology (GO) analyses in the DAVID (<https://david.ncifcrf.gov/>) and PlasmoDB databases (<http://plasmodb.org/plasmo/>) for host and parasite proteins, respectively. The relationships between GO terms were visualized using the Cytoscape 3.3.0 software with the ClueGO plugin (Wang et al., 2015). The GO analyses were conducted using a right-sided hypergeometric test with Benjamini-Hochberg correction; values were considered to be significant when the *P* value was less than 0.05. The GO term levels were set from one to eight. The minimum number of genes to form a cluster was set at two, while the minimum percentage of genes covered by our dataset against the database was set at 1%. The rest of the setting were left as defaults. The resultant Fig. 2A shows the top GO terms (cellular components) of the parasite-derived 88 *SBP1*-interacting factors identified in Table S3, whereas Fig. 2B shows the relationships between the top GO terms.

### ***SDS-PAGE and western blotting.***

Protein extracts from parasite-infected RBCs were separated by SDS-PAGE in gradient precast 5%–20% polyacrylamide gels (e-PAGEL, E-R520L; ATTO), and blotted onto PVDF membranes (Bio-Rad). Membranes were probed with primary antibodies at the following dilutions (in 5% blocking agent in PBS): rabbit anti-SBP1, 1/5000; mouse anti-SBP1, 1/1000; mouse anti-FLAG, 1/1000; rabbit anti-EXP2, 1/2000; mouse anti-spectrin, 1/20; rabbit anti-STOM, 1/100; rabbit anti-KPNB1, 1/400; mouse anti-MPP1, 1/20. Mouse anti-sera obtained in this study were used at dilutions ranging from 1/10 to 1/500. Secondary antibodies were horseradish peroxidase (HRP)-conjugated goat anti-mouse and goat anti-rabbit, both used at 1/1000.

### ***Live fluorescence and immunofluorescence.***

Live cell imaging assays were conducted as described previously (Heiber et al., 2013). The parasite nuclei were stained with 1  $\mu$ g/ml DAPI (Invitrogen) for 30 min at RT. Indirect

immunofluorescent assays were conducted either on blood smears on glass slides (Maier et al., 2008) or by using an alternative method (Tonkin et al., 2004). In the latter method, the cells were washed in PBS once, and fixed with 4% paraformaldehyde (Wako) and 0.0075% glutaraldehyde (Wako) in PBS for 30 min at RT. After centrifugation and being washed with PBS twice, the cells were permeabilized with 0.1% Triton X-100 (Sigma) in PBS for 10 min at RT. After centrifugation and being washed in PBS, the samples were blocked with blocking reagent (Blocking One, Nacalai Tesque) for 1 h at RT, and incubated with primary antibodies in 5% blocking reagent in PBS for 1 h at RT. They were then rinsed with 0.1% Tween 20 in PBS (PBS-T) three times, and incubated with secondary antibodies for 1 h at RT. Finally, the samples were washed three times in PBS-T and mounted on glass slides with mounting medium (Dako). Coverslips were then inverted onto the glass slides, which were subsequently observed under the Leica TCS SP5 II confocal laser microscope equipped with a 100X/1.4 numerical aperture oil immersion lens. Images were collected and processed with LAS AF software (Leica).

### ***Time course analysis.***

To determine the expression and localization of parasite proteins in the asexual stage of parasite development, time course analysis was performed as previously described (Rug et al., 2014). Briefly, cells were tightly synchronized by repeated D-sorbitol treatment (Lambros and Vanderberg, 1979), and subjected to either immunofluorescence or western blot analyses. For the latter, cell samples (50 µl of packed iRBCs, 5%–10% parasitemia) were taken every 8 hours after invasion from the same culture dish. The cells were lysed with 0.09% saponin in PBS for 15 min on ice, thoroughly washed with PBS three times, and cell pellets were completely dissolved in 50 µl of 4% SDS/0.5% Triton X-100/0.5 × PBS. Then, 50 µl of the cell lysate was mixed with the same volume of 2 × SDS sample buffer, boiled for 5 min, and subsequently subjected to SDS/PAGE followed by western blot analysis.

### ***Subcellular fractionation assay.***

To define the protein subcellular localization, selective permeabilization assays on parasite-infected RBCs were conducted (Boddey et al., 2016; Gruring et al., 2012), with some modifications. Briefly, iRBCs were MACS-purified, washed with PBS once, and lysed with 5 U/ml tetanolysin (List biological Lab.) in PBS for 20 min at 37 °C. After centrifugation for 5 min at 15,000 rpm, the tetanolysin pellet was washed with PBS once, and further sequentially lysed with 0.03% saponin (Sigma) in PBS for 20 min on ice. After centrifugation, the resultant pellet was washed with PBS twice, and dissolved in 4% SDS/0.5% Triton X-100/0.5 × PBS. Equivalent amounts of supernatants and pellet were analyzed by western blotting.

### **Cytoadherence assays.**

The adhesive properties of iRBCs to the receptor CD36 were quantified using static-based assays as described previously (Beeson et al., 1999; Beeson et al., 1998; Janes et al., 2011; Oberli et al., 2016; Saito et al., 2017). Briefly, 5  $\mu$ l of recombinant human CD36 (100  $\mu$ g/ml, R&D systems) was immobilized on 90  $\times$  15-mm polystyrene dishes (Sansei Medical Co., Ltd., Kyoto) and incubated overnight at 4  $^{\circ}$ C in a humid container. The protein spots were then blocked with 1% BSA in PBS for 30 min at room temperature and washed twice with pre-warmed protein binding medium (RPMI-1640 medium containing 0.1% bovine serum albumin). Trophozoite- or schizont-infected erythrocytes were purified by gelatin sedimentation, resuspended to 0.5% hematocrit in protein binding medium, then spotted onto immobilized proteins, and incubated for 30 min at 37  $^{\circ}$ C. Prior to binding assays, parasite cultures were subjected to gelatin sedimentation three times to enrich for knob-positive parasites as described elsewhere (Dixon et al., 2017). Unbound erythrocytes were removed by gently flooding each spot with binding medium, rocking the dish back and forth, then pouring off and replacing the medium five times. Bound cells were then fixed with 2% glutaraldehyde in PBS for 2 h at room temperature, stained with DAPI overnight, and counted by using a fluorescence microscope (BZ-X700, KEYENCE, Tokyo, Japan). The number of infected erythrocytes bound to the receptor was determined by counting ten fields using a 30 $\times$  objective and is expressed as a ratio relative to the number of *P. falciparum* 3D7-infected erythrocytes.

### **Growth and invasion assay.**

Growth and invasion assays were performed as previously described (Baldi et al., 2000; Reed et al., 2000), with some modifications. For growth assay, tightly synchronized ring stage parasites were added to fresh erythrocytes at a final parasitemia of 0.3%, and hematocrit of 0.5% in 1 mL of culture medium in the absence or presence of drugs. The final concentrations of each drug in medium were: 20 U/mL for heparin (Novo heparin, Mochida Pharmaceutical, Tokyo, Japan), and 20  $\mu$ M for pyrimethamine (Sigma). The medium was changed daily, and the parasitemia were counted by blood smear every 24 hours post-incubation for 2 cycles of parasite growth. For the invasion inhibition assay, parasite cultures were tightly synchronized with a cycle window of 3 hours, and MACS-purified schizont cultures were added to fresh erythrocytes at a final parasitemia of 0.4% or 5% for parasitemia count or indirect immunofluorescence analyses, respectively. Thin blood smears were prepared at 1, 3, and 6 hours post-invasion, and were subsequently analyzed for further experiments.

### **Electron microscopy.**

Scanning electron microscopy (SEM) was performed as previously described (Rug et al., 2006).

The infected RBCs were purified by gelatin flotation, washed with PBS twice, and fixed with glutaraldehyde (2% in PBS) for 30 min at RT. The erythrocytes were then washed with PBS twice, and settled onto APS-coated glass slides (Matsunami Glass Inc., Ltd., Osaka, Japan) for 30 min. The cells were washed three times in 0.1 M PB (pH 7.4), and further fixed in osmium tetroxide (1% in 0.1 M PB) for 30 min at RT. After fixation, the cells were dehydrated in an ascending series of ethanol (70%, 80%, 90%, 95%, 100%, 3×100%; 5 min each), transferred into 2-Methyl-2-propanol, and dried in a freeze dryer (ES-2030; Hitachi Koki Co., Ltd., Tokyo, Japan). The dried samples were coated with platinum-palladium in an ion sputtering device (E1010; Hitachi Koki Co., Ltd.), and observed with the SE mode of a field emission SEM (S-4100; Hitachi High Technologies).

Transmission electron microscopy (TEM) was performed as previously described (Rug et al., 2006), and samples were viewed in an HT7700 transmission electron microscope (Hitachi, Tokyo, Japan). Immunoelectron microscopic examination (IEM) by TEM was conducted as previously described (Tonkin et al., 2004; Rug et al., 2014). Briefly, the infected RBCs were purified by Percoll gradient or gelatin floatation, washed with PBS once, and fixed with 2% paraformaldehyde (Wako) in PBS for 10 min at RT. The cells were then washed in PBS three times, and permeabilized with 10 U/ml tetanolysin for 20 min at 37 °C. They were then washed in PBS twice and re-fixed with 4% paraformaldehyde and 0.0075% glutaraldehyde (Wako) in PBS for 30 min at RT. Then, the cells were washed in PBS twice, blocked with blocking reagent (Blocking One, Nacalai Tesque) for 1 h at RT, and incubated with primary antibodies for 1 h at RT. They were then rinsed with 0.1% Tween 20 in PBS (PBS-T) three times, and incubated with the appropriate secondary antibody conjugated with gold nanoparticles for 1 h at RT. The cells were rinsed again in PBS-T three times, and post-fixed with 2.0% glutaraldehyde in 0.1 M sodium cacodylate buffer and then with 1% OsO<sub>4</sub> in 0.1 M phosphate buffer (pH 7.4) for 30 min at RT. Then, the cells were serially dehydrated and embedded in LR White resin (London Resin Company Ltd., London, UK). Ultrathin sections (90-nm thick) were cut and examined using an HT7700 transmission electron microscope without uranyl acetate or lead citrate staining.

### ***Phylogenetic analyses.***

To investigate the phylogenetic relationships among genes containing the alpha/beta hydrolase domain, the protein sequences coding alpha/beta hydrolase were retrieved from the PlasmoDB database, and were phylogenetically analyzed as previously described (Takano et al., 2009). Maximum likelihood analyses were carried out on the protein regions encoding the alpha/beta hydrolase domain. Bootstrap support values were calculated from 1000 replicates using maximum likelihood and the preferred model of evolution (Takano et al., 2009). To investigate the similarity of gene expression in the intraerythrocytic stage of the parasites, gene expression

data of DeRisi's microarrays were retrieved from PlasmoDB. Hierarchical clustering analyses of the gene expression profiles of the 205 proteins in Table S2 were performed on R software ver. 2.15.2. (<https://www.r-project.org/>) as described elsewhere (Langfelder and Horvath, 2008).

### ***Statistical tests.***

All statistical analyses were performed by using R software ver. 2.15.2 (<https://www.r-project.org/>). If not specified, all statistical analyses used one-way ANOVA with Tukey's post-hoc test (normal distribution assumed). For all statistical tests, values were considered to be significantly different when the  $P$  value was less than 0.05.

## Supplemental References

- Baldi, D.L., Andrews, K.T., Waller, R.F., Roos, D.S., Howard, R.F., Crabb, B.S., and Cowman, A.F. (2000). RAP1 controls rhoptry targeting of RAP2 in the malaria parasite *Plasmodium falciparum*. *Embo J* 19, 2435-2443.
- Batinovic, S., McHugh, E., Chisholm, S.A., Matthews, K., Liu, B., Dumont, L., Charnaud, S.C., Schneider, M.P., Gilson, P.R., de Koning-Ward, T.F., *et al.* (2017). An exported protein-interacting complex involved in the trafficking of virulence determinants in *Plasmodium*-infected erythrocytes. *Nat Commun* 8, 16044.
- Beeson, J.G., Brown, G.V., Molyneux, M.E., Mhango, C., Dzinjalama, F., and Rogerson, S.J. (1999). *Plasmodium falciparum* isolates from infected pregnant women and children are associated with distinct adhesive and antigenic properties. *J Infect Dis* 180, 464-472.
- Beeson, J.G., Chai, W., Rogerson, S.J., Lawson, A.M., and Brown, G.V. (1998). Inhibition of binding of malaria-infected erythrocytes by a tetradecasaccharide fraction from chondroitin sulfate A. *Infect Immun* 66, 3397-3402.
- Boddey, J.A., O'Neill, M.T., Lopaticki, S., Carvalho, T.G., Hodder, A.N., Nebl, T., Wawra, S., van West, P., Ebrahimzadeh, Z., Richard, D., *et al.* (2016). Export of malaria proteins requires co-translational processing of the PEXEL motif independent of phosphatidylinositol-3-phosphate binding. *Nat Commun* 7, 10470.
- Crabb, B.S., Triglia, T., Waterkeyn, J.G., and Cowman, A.F. (1997). Stable transgene expression in *Plasmodium falciparum*. *Mol Biochem Parasitol* 90, 131-144.
- Dixon, M.W., Kenny, S., McMillan, P.J., Hanssen, E., Trenholme, K.R., Gardiner, D.L., and Tilley, L. (2017). Genetic ablation of a Maurer's cleft protein prevents assembly of the *Plasmodium falciparum* virulence complex. *Mol Microbiol* 81, 982-993.
- Duraisingh, M.T., Triglia, T., and Cowman, A.F. (2002). Negative selection of *Plasmodium falciparum* reveals targeted gene deletion by double crossover recombination. *Int J Parasitol* 32, 81-89.
- Gorai, T., Goto, H., Noda, T., Watanabe, T., Kozuka-Hata, H., Oyama, M., Takano, R., Neumann, G., Watanabe, S., and Kawaoka, Y. (2012). F1Fo-ATPase, F-type proton-translocating ATPase, at the plasma membrane is critical for efficient influenza virus budding. *Proc Natl Acad Sci U S A* 109, 4615-4620.
- Gruring, C., Heiber, A., Kruse, F., Flemming, S., Franci, G., Colombo, S.F., Fasana, E., Schoeler, H., Borgese, N., Stunnenberg, H.G., *et al.* (2012). Uncovering common principles in protein export of malaria parasites. *Cell Host Microbe* 12, 717-729.
- Heiber, A., Kruse, F., Pick, C., Gruring, C., Flemming, S., Oberli, A., Schoeler, H., Retzlaff, S., Mesen-Ramirez, P., Hiss, J.A., *et al.* (2013). Identification of new PNEPs indicates a substantial non-PEXEL exportome and underpins common features in *Plasmodium falciparum* protein export. *PLoS Pathog* 9, e1003546.
- Janes, J.H., Wang, C.P., Levin-Edens, E., Vigan-Womas, I., Guillotte, M., Melcher, M.,

Mercereau-Puijalon, O., and Smith, J.D. (2011). Investigating the host binding signature on the *Plasmodium falciparum* PfEMP1 protein family. *PLoS Pathog* 7, e1002032.

Jensen, J.B. (1978). Concentration from continuous culture of erythrocytes infected with trophozoites and schizonts of *Plasmodium falciparum*. *Am J Trop Med Hyg* 27, 1274-1276.

Knuepfer, E., Rug, M., Klonis, N., Tilley, L., and Cowman, A.F. (2005). Trafficking of the major virulence factor to the surface of transfected *P. falciparum*-infected erythrocytes. *Blood* 105, 4078-4087.

Kramer, K.J., Kan, S.C., and Siddiqui, W.A. (1982). Concentration of *Plasmodium falciparum*-infected erythrocytes by density gradient centrifugation in Percoll. *J Parasitol* 68, 336-337.

Lambros, C., and Vanderberg, J.P. (1979). Synchronization of *Plasmodium falciparum* erythrocytic stages in culture. *J Parasitol* 65, 418-420.

Langfelder, P., and Horvath, S. (2008). WGCNA: an R package for weighted correlation network analysis. *BMC Bioinformatics* 9, 559.

Maier, A.G., Rug, M., O'Neill, M.T., Brown, M., Chakravorty, S., Szeszak, T., Chesson, J., Wu, Y., Hughes, K., Coppel, R.L., *et al.* (2008). Exported proteins required for virulence and rigidity of *Plasmodium falciparum*-infected human erythrocytes. *Cell* 134, 48-61.

Mantel, P.Y., Hoang, A.N., Goldowitz, I., Potashnikova, D., Hamza, B., Vorobjev, I., Ghiran, I., Toner, M., Irimia, D., Ivanov, A.R., *et al.* (2013). Malaria-infected erythrocyte-derived microvesicles mediate cellular communication within the parasite population and with the host immune system. *Cell Host Microbe* 13, 521-534.

Marti, M., Good, R.T., Rug, M., Knuepfer, E., and Cowman, A.F. (2004). Targeting malaria virulence and remodeling proteins to the host erythrocyte. *Science* 306, 1930-1933.

Oberli, A., Zurbrugg, L., Rusch, S., Brand, F., Butler, M.E., Day, J.L., Cutts, E.E., Lavstsen, T., Vakonakis, I., and Beck, H.P. (2016). *Plasmodium falciparum* *Plasmodium* helical interspersed subtelomeric proteins contribute to cytoadherence and anchor *P. falciparum* erythrocyte membrane protein 1 to the host cell cytoskeleton. *Cell Microbiol* 18, 1415-1428.

Reed, M.B., Caruana, S.R., Batchelor, A.H., Thompson, J.K., Crabb, B.S., and Cowman, A.F. (2000). Targeted disruption of an erythrocyte binding antigen in *Plasmodium falciparum* is associated with a switch toward a sialic acid-independent pathway of invasion. *Proc Natl Acad Sci U S A* 97, 7509-7514.

Ribaut, C., Berry, A., Chevalley, S., Reybier, K., Morlais, I., Parzy, D., Nepveu, F., Benoit-Vical, F., and Valentin, A. (2008). Concentration and purification by magnetic separation of the erythrocytic stages of all human *Plasmodium* species. *Malar J* 7, 45.

Rug, M., Cyrklaff, M., Mikkonen, A., Lemgruber, L., Kuelzer, S., Sanchez, C.P., Thompson, J., Hanssen, E., O'Neill, M., Langer, C., *et al.* (2014). Export of virulence proteins by malaria-infected erythrocytes involves remodeling of host actin cytoskeleton. *Blood* 124, 3459-3468.

Rug, M., Prescott, S.W., Fernandez, K.M., Cooke, B.M., and Cowman, A.F. (2006). The role of KAHRP domains in knob formation and cytoadherence of *P falciparum*-infected human erythrocytes. *Blood* 108, 370-378.

Saito, F., Hirayasu, K., Satoh, T., Wang, C.W., Lusingu, J., Arimori, T., Shida, K., Palacpac, N.M.Q., Itagaki, S., Iwanaga, S., *et al.* (2017). Immune evasion of *Plasmodium falciparum* by RIFIN via inhibitory receptors. *Nature* 552, 101-105.

Takano, R., Nidom, C.A., Kiso, M., Muramoto, Y., Yamada, S., Sakai-Tagawa, Y., Macken, C., and Kawaoka, Y. (2009). Phylogenetic characterization of H5N1 avian influenza viruses isolated in Indonesia from 2003-2007. *Virology* 390, 13-21.

Tonkin, C.J., van Dooren, G.G., Spurck, T.P., Struck, N.S., Good, R.T., Handman, E., Cowman, A.F., and McFadden, G.I. (2004). Localization of organellar proteins in *Plasmodium falciparum* using a novel set of transfection vectors and a new immunofluorescence fixation method. *Mol Biochem Parasitol* 137, 13-21.

Trager, W., and Jensen, J.B. (2005). Human malaria parasites in continuous culture. 1976. *J Parasitol* 91, 484-486.

Tsuboi, T., Takeo, S., Iriko, H., Jin, L., Tsuchimochi, M., Matsuda, S., Han, E.T., Otsuki, H., Kaneko, O., Sattabongkot, J., *et al.* (2008). Wheat germ cell-free system-based production of malaria proteins for discovery of novel vaccine candidates. *Infect Immun* 76, 1702-1708.

Waller, K.L., Muhle, R.A., Ursos, L.M., Horrocks, P., Verdier-Pinard, D., Sidhu, A.B., Fujioka, H., Roepe, P.D., and Fidock, D.A. (2003). Chloroquine resistance modulated in vitro by expression levels of the *Plasmodium falciparum* chloroquine resistance transporter. *J Biol Chem* 278, 33593-33601.

Wang, J., Zhang, C.J., Chia, W.N., Loh, C.C., Li, Z., Lee, Y.M., He, Y., Yuan, L.X., Lim, T.K., Liu, M., *et al.* (2015). Haem-activated promiscuous targeting of artemisinin in *Plasmodium falciparum*. *Nat Commun* 6, 10111.

Watanabe, T., Kawakami, E., Shoemaker, J.E., Lopes, T.J., Matsuoka, Y., Tomita, Y., Kozuka-Hata, H., Gorai, T., Kuwahara, T., Takeda, E., *et al.* (2014). Influenza virus-host interactome screen as a platform for antiviral drug development. *Cell Host Microbe* 16, 795-805.